Journal of Physiology (1993), **461**, *pp.* 339–378
With 17 figures
Printed in Great Britain

A STATISTICAL ANALYSIS OF ACETYLCHOLINE RECEPTOR ACTIVATION IN *XENOPUS* MYOCYTES: STEPWISE *VERSUS* CONCERTED MODELS OF GATING

BY ANTHONY AUERBACH

From the Department of Biophysical Sciences, State University of New York at Buffalo, Buffalo, NY 14214, USA

(*Received 27 September 1991*)

SUMMARY

1. The kinetic properties of single channel currents from fetal-type acetylcholine receptors in embryonic *Xenopus* myocytes (60 h old) have been analysed by a maximum-likelihood method.

2. At very high acetylcholine (ACh) concentrations (up to 5 mM) the effective opening rate appears to saturate at $\sim 30000\ s^{-1}$.

3. The kinetics were analysed according to the standard *concerted* scheme that postulates a single channel-opening conformational change after two agonists are bound, and a rarely invoked *stepwise* scheme that postulates semi-independent conformational changes in two distinct gating domains. Both models assume that agonist cannot escape from a channel (or domain) that is in its activated conformation.

4. With either activation scheme the kinetic analyses indicate that ACh binds at a rate of $\sim 2 \times 10^8\ s^{-1}\ M^{-1}$ and dissociates from doubly liganded receptors at a rate of $\sim 28000\ s^{-1}$, and that the activation process is asymmetric, i.e. the binding (concerted model) or gating (stepwise model) transitions are not equal and independent.

5. In eighteen of twenty-seven file-by-file comparisons, the likelihood of the stepwise model was greater than that of the concerted model. In seven such comparisons, the likelihood of the concerted model was greater than that of the stepwise model, and in two there was no difference. Log likelihood ratio distributions were obtained from three files (those with the most events) by multiple cycles of resampling and fitting. The means of these distributions were significantly greater than zero, indicating that the stepwise scheme was as good as, or better than, the concerted scheme in describing receptor activation.

6. According to the stepwise view, two binding sites must be occupied and two 'gates' activated for conduction to occur. Although equivalent binding is not an essential aspect of stepwise activation, the binding sites can be identical and have a low affinity for ACh ($K_d \sim 130\ \mu M$). Either the isomerization rates of the gating domains are different, or they are influenced by the conformational status of its counterpart, with activation increasing ~ 3-fold and deactivation decreasing ~ 10-fold if the complementary domain is in the active conformation. Stepwise

MS 9771

activation predicts that the decay of the endplate current is determined by five rates.

INTRODUCTION

The kinetic properties of neuromuscular acetylcholine (ACh) receptors have been actively investigated since Fatt & Katz (1952) first noted the exponential decay of the endplate current. In 1957, del Castillo & Katz proposed a model for receptor activation:

$$C \underset{k_-}{\overset{[A]k_+}{\rightleftarrows}} AC \underset{\alpha}{\overset{\beta}{\rightleftarrows}} AO. \qquad \text{Model (1)}$$

According to this scheme, a closed, vacant receptor (C) binds ACh (A) and remains closed (AC) until changing to an open conformation (AO) from which agonist does not dissociate (α and β are channel closing and opening rate constants, respectively; k_+ and k_- are the association and dissociation rate constants, respectively).

Since the model was first put forth, this basic kinetic scheme has been expanded in several significant ways. Channel opening usually follows the binding of two agonist molecules, rather than just one (Katz & Thesleff, 1958). Vacant and monoliganded channels, too, can open (Jackson, 1986). ACh itself can block ionic conduction (Sine & Steinbach, 1984; Ogden & Colquhoun, 1985). Despite these modifications, the essential features of the model have remained unchanged for 35 years, i.e. ACh receptors open in response to binding agonists, binding and gating are distinct processes, and agonist molecules do not readily dissociate from open channels.

Although substantial effort has gone into cholinergic receptor kinetic analysis, a consensus as to the rates of binding and gating has been elusive. Different preparations and methods of obtaining rate estimates have been employed, current components have been misidentified, and the effects of limited bandwidth have gone unadvertised. There is now agreement that for frog (Colquhoun & Sakmann, 1985; Colquhoun & Odgen, 1988), BC_3H_1 cell (Liu & Dilger, 1991; Maconochie & Steinbach, 1992) and *Torpedo* (Sine, Claudio & Sigworth, 1990) receptors the opening rate of the most common form of cholinergic channel is fast, i.e. close to the time resolution of the instrumentation. In addition, a substantial difference in the affinities of the two agonist binding sites has been suggested for mouse muscle (Jackson, 1988), *Torpedo* (Sine *et al.* 1990) ACh and BC_3H_1 cell (Blount & Merlie, 1989) receptors.

Here I describe the kinetic properties of single ACh-activated channels in embryonic *Xenopus* myocytes elicited over a wide range of agonist concentrations and analysed by the maximum-likelihood method of Horn & Lange (1983). The data are discussed in terms of two different models of receptor activation: the usual *concerted* scheme, where the conformational change in the channel protein that results in ionic conduction occurs in an all-or-none fashion after two agonist molecules are bound, and a more rarely invoked *stepwise* scheme, where each gating domain semi-independently changes its conformation after binding an agonist molecule, with ionic conduction taking place only when both domains have isomerized. This scheme gives rise to an apparent negative co-operativity in the affinities of the two ACh molecules even though association and dissociation rates can

be identical at both sites. Some results have been presented in abstract form (Auerbach, 1992).

METHODS

Cell preparation. Dorsal portions of stage 20–22 *Xenopus* embryos were treated with 0·1 % collagenase for 30 min at 24 °C. Myotomal muscle cells were isolated with fine needles, treated for 5 min in 0·1 % trypsin, and plated onto plastic culture dishes. The cells were maintained in culture (60 % Leibowitz–0·5 % horse serum) at 24 °C for 30–40 h. Sometimes, the cells were transferred to a 10 °C incubator for an additional 24 h before use. The average age of the cells at the time of channel recording was ~ 60 h, or the equivalent of stage 66 (Nieuwkoop & Faber, 1967). The culture medium was exchanged with physiological saline ((mM): 110 NaCl, 2 KCl, 1 $CaCl_2$, 10 NaHepes, pH 7·4) before use. The temperature for all electrophysiology experiments was 18 °C.

Patch clamp experiments. All results are from cell-attached patches. For experiments at single agonist concentrations, pipettes (borosilicate glass) were filled with saline solution plus AChCl (Sigma Chemical Co., St Louis, MO, USA). For backfilled pipette experiments (Auerbach, 1991), pipette-tip regions were filled by capillary action with drug-free saline, and were then backfilled with ACh-containing saline. The tip-filling procedure was monitored with videomicroscopy and the height of this region (L) was measured with an accuracy of 25 μM. The backfilling was always done so that a small bubble was trapped between tip and shank regions so that the filling did not stir the interface. A stopwatch was started the moment the bubble was dislodged by flicking the pipette, and the time required to form a seal was noted (typically 60–90 s). The concentration of ACh at the tip ($[A]_t$) was computed according to the equation that describes diffusion in a cone:

$$[A]_t = [A][1 + 2\Sigma(-1)^n \exp(-n^2 t/\tau)] \quad \text{and} \tag{1a}$$

$$\tau = L^2/\pi D, \tag{1b}$$

where [A] is the shank (steady-state) concentration of ACh, t is the time (s) elapsed from dislodging the bubble, L is the fill height (cm), and D is the diffusion constant of ACh ($0{\cdot}6 \times 10^{-5}$ M^{-1} s^{-1}; Dionne, 1976).

An Axopatch 1B clamp (Axon Instruments, Foster City, CA, USA) was used to amplify the channel currents, which were filtered at 20 kHz (−3 dB; 8-pole Bessel) and stored on a digital data recorder (94 kHz sampling; Instrutech VR-10, Mineola, NY, USA).

Data acquisition and event detection. The data were played back into a 386-based computer as an analog signal with redigitization at 50 kHz (FETCHEX; Axon Instruments), or directly through a digital interface (VR-111; Instrutech) at 47 kHz. Records were digitally filtered (Gaussian low-pass filter; net effective frequency 3–7 kHz) and single channel currents were detected with a half-amplitude crossing algorithm (IPROC; Sachs, Neil & Barkakati, 1982) that estimated transition times to a precision of 2 μs by using linear interpolation between samples. No corrections were made to the durations of brief events. To eliminate extraneous currents and to ensure a consistent detection threshold, bursts were required to have an amplitude that fell within 0·5 pA of the mean value. To summarize: the sampling interval was 20 μs, the system dead time was 24–56 μs (typically 35 μs), and the duration resolution was 2 μs.

Kinetic analysis. The kinetic properties of the predominant, fetal-type cholinergic channel (Auerbach & Lingle, 1987) were analysed by the Horn & Lange (1983) maximum-likelihood method. This involves computing the likelihood of observing the experimental data given a kinetic model and adjusting the parameters of the model until the likelihood is maximal (until the −log likelihood is at a minimum). This approach has been used to study single Na^+ channels (Horn & Vandenberg, 1984) and glutamate-receptor channels (Bates, Sansom, Ball, Ramsey & Usherwood, 1990).

First, a burst-oriented analysis of the currents was carried out in order to select an apparently homogeneous set (LPROC; Neil, Xiang & Auerbach, 1991). Bursts were defined as a group of open intervals separated by closures less than some critical value, τ_c. Note that at high ACh concentrations, such an assembly of open and closed intervals is sometimes called a 'cluster'. In order to define τ_c, log bin-width histograms (Sigworth & Sine, 1987) were constructed of all closed intervals in the record. At all ACh concentrations, more than 70 % of closed intervals belonged to one exponentially distributed component; τ_c was set to be 3–5 times the time constant of this component.

Once defined, a subset of bursts was selected for further analysis according to the following

criteria: mean amplitude, number of open intervals (> 4), mean open interval duration, and probability of being open. The ranges used for each of these parameters were determined by examining the means and variances for the entire record. This selection procedure reduced the contribution of currents from dissimilar conductance and kinetic forms of cholinergic receptor (Auerback & Lingle 1986), but also reduced the number of bursts that were analysed for each record.

Once a subset of bursts was selected, a list of the durations of open and closed intervals within those bursts were made. In backfilled patch pipettes, this list contained the estimated ACh concentration at the time the interval occurred, computed according to eqn (1). Each burst represents the kinetics of one receptor. Thus, even though the patch contained more than one channel, the likelihood function was computed as if the currents came from one channel.

Bursts were assumed to be independent, and the log likelihood for a record was the sum of the log likelihoods for each burst. Models had a single open state; because, by definition, bursts begin with an opening, bursts were assumed to start in the open state.

The rates of the model define a transition matrix (Q) that may be used to compute the probability of moving between states of the model in time t (Colquhoun & Hawkes, 1982). Two modifications of this transition matrix were carried out prior to the likelihood computation.

First, the rates of the agonist association steps were defined as the product of the ACh concentration and an intrinsic rate. The corresponding elements of Q were therefore multiplied by the concentration of agonist. For single-concentration patches, this was carried out once for each file. For backfilled patch experiments, the Q matrix was updated for each burst.

The second modification to Q was required because brief open or closed sojourns will not be detected and will cause the experimentally obtained interval durations to deviate from those predicted by the kinetic model. To correct for these 'missed events', Q was modified according to the first-order correction of Roux & Sauve (1985) (R. Horn, unpublished results):

$$Q^* = M + T \exp(A\tau_m),$$

where Q* is the modified Q matrix, τ_m is the minimum duration that is detected (the system 'dead time'), and M, A, and T are matrices defined in Roux & Sauve. This modification was carried out once for each parameter set. In the computation of the likelihood, matrix exponentials were computed by solving the eigenvectors and eigenvalues of Q*. The use of this correction sometimes created an instability in the fitting procedure. The correction was useful only under conditions where long open intervals were interrupted by short-lived gaps.

In practice, because of noise τ_m is not a sharp limit and intervals as short as 2 μs, more than 17 times shorter than the typical dead time, were entered into the list of event durations. Therefore, in order to insure that the modified Q matrix was appropriate to the data, intervals in the data file that were shorter than the τ_m value used to correct Q were omitted and the adjacent intervals were joined.

Optimization was achieved by the Simplex method (Nelder & Mead, 1965). Rates of the model could be fixed or defined as multiples of other rates, thus limiting the number of free parameters in the fit. The standard errors of the parameter estimates were obtained either from the 0·5-unit likelihood intervals obtained by bisection (Colquhoun & Sigworth, 1983), or from the standard deviation of the distribution of parameter estimates obtained by resampling the original data set (Horn, 1987). Other curve fitting was done with the programs NFITS (C. Lingle, Washington University, St Louis, USA) or NFIT (Island Products, Galveston, TX, USA).

A typical data set might have thirty bursts and 2500 open and closed intervals; the models I have used have from four to eight states, and from three to five free parameters. For a given problem, the time required to get an estimate on the rates and their standard errors (a substantial part of the computation) depended on the starting estimates but were typically several hours on a 1 MFLOP Sun Sparcstation.

Resampling and simulation. Resampling was used to determine the significance of the log likelihood ratios (LLR) obtained by fitting each record to different models (Horn, 1987). The original list of n interval durations was resampled with replacement on a burst-by-burst basis (to maintain any time-dependent intraburst structure) until exactly n intervals had been selected. If the original data was from a backfilled patch experiment, the relevant ACh concentration for each burst was used to scale the association rates of Q* on a burst-by-burst basis. The resampled file was fitted by two different kinetic models, and the parameter estimates and log likehood values were

compiled for each fit to each model. Files were resampled and fit 30–400 times. The distributions of parameter values, and of the LLR estimates for each resampled list were used to determine standard errors on these values.

Simulation was used to test if stepwise and concerted models were distinguishable under typical experimental conditions. Exponentially distributed interval durations were computed according to the transition matrix, and bursts of currents approximately 200 ms in duration were generated at a sampling interval of 20 μs. Filtering was achieved by using a filtered step response at the transitions between states of differing currents (Magelby & Weiss. 1990). Gaussian white noise was added to the record, and events were detected by a half-amplitude crossing criterion (no interpolation).

Rate verification. Once a set of rates was obtained, the open and closed interval probability density functions (pdf) were computed (Colquhoun & Hawkes, 1982). As with the likelihood computation, the effects of limited bandwidth were considered by modifying the transition matrix. The effects of the enforced dead time on the relative contribution of each component was taken into account (Crouzy & Sigworth, 1990). The pdfs were scaled by the number of (open or closed) intervals in the record, and were superimposed on one-dimensional interval duration histograms.

RESULTS

Models of receptor activation

ACh causes nicotinic receptors to open. It is logical, but not mandatory, to assume that ligand binding and channel opening are kinetically separable steps. In the single-ligand activation model of del Castillo & Katz (1957) (model (1)) there is the additional assumption that agonist molecules do not dissociate from an open channel.

There is extensive biochemical, structural, and pharmacological data that indicate that neuromuscular ACh receptors have two ACh binding sites and one permeation pathway, and that usually ions permeate the channel only after two agonists are bound. One possible mode of operation, then, is that vacant and monoliganded receptors are in a 'closed' channel conformation, and that the transition from a 'closed' to an 'open' channel occurs as a single step only after receptors become doubly liganded. Accordingly to this view, the opening of a channel is a highly *concerted* process, i.e. a channel isomerizes as a whole after binding two agonists. This view has become the standard kinetic model for cholinergic receptor activation:

$$\mathrm{C} \underset{k_{-1}}{\overset{[\mathrm{A}]k_{+1}}{\rightleftharpoons}} \mathrm{AC} \underset{k_{-2}}{\overset{[\mathrm{A}]k_{+2}}{\rightleftharpoons}} \mathrm{A_2C} \underset{\alpha}{\overset{\beta}{\rightleftharpoons}} \mathrm{AO}. \qquad \text{Model (2)}$$

As with the del Castillo & Katz scheme (model (1)), this scheme proposes that agonist molecules cannot dissociate from open channels. The concerted scheme is a two-state (closed–open) version of the Monod–Wyman–Changeaux (MWC) model of allosterism (Monod, Wyman & Changeaux, 1965; Wyman & Gill, 1990).

Another way of extending model (1) to incorporate multiple agonist binding sites and sigmoidal dose–response characteristics is to assume stepwise activation of separate gating domains of the channel. After binding an agonist molecule, a domain shifts from a resting to an 'active' conformation, but the channel becomes conductive to ions only when all (or in the case of AChR, two) domains are 'active':

$$\mathrm{C} \underset{k_-}{\overset{2[\mathrm{A}]k_+}{\rightleftharpoons}} \mathrm{AC} \underset{\alpha_1}{\overset{\beta_1}{\rightleftharpoons}} \mathrm{AC^*} \underset{k_-}{\overset{[\mathrm{A}]k_+}{\rightleftharpoons}} \mathrm{A_2C^*} \underset{\alpha}{\overset{\beta}{\rightleftharpoons}} \mathrm{A_2O}. \qquad \text{Model (3)}$$

where * indicates a channel with only one 'active' domain (β_1 and α_1 are the opening and closing rates of the first domain to activate). Again, this model assumes that agonist does not dissociate from an 'active' domain.

This scheme may be called a *stepwise* model of cholinergic receptor activation because channel opening results from the sequential (but random) activation of two

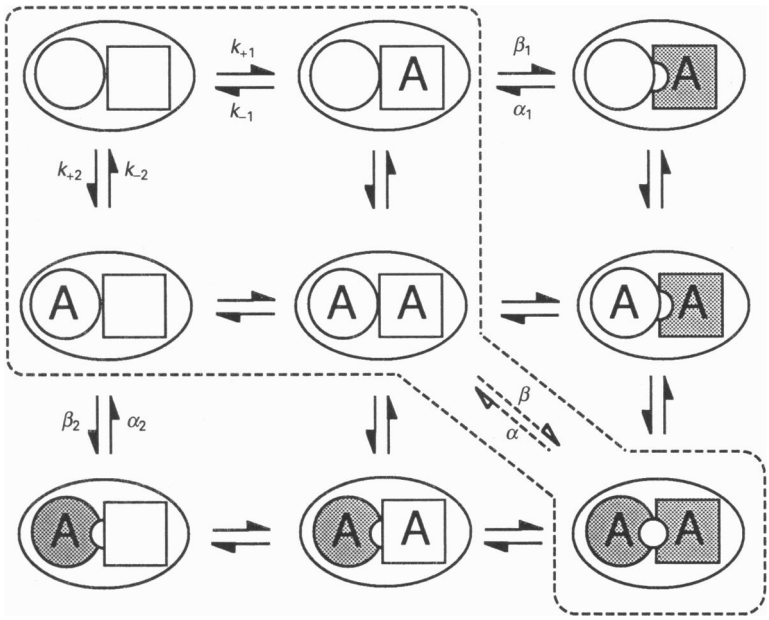

Fig. 1. Models of receptor activation. The ovals are receptor–channel complexes, and the circles and squares are domains that each can be in one of three conformations: resting–vacant, resting–occupied (by agonist A), or activated–occupied (shaded). The full matrix of states is a stepwise activation model, with conduction possible only when both domains are active. The outlined states constitute a concerted activation model, which has an added transition between the two doubly liganded forms of the receptors. Both models assume that agonist cannot dissociate from an active domain. Some rates have been left out for clarity. Linear versions of both models are given in the text.

distinct gates. It is derived from the induced fit or Koshland–Nemethy–Filmer (KNF) model of allosterism (Koshland, Nemethy & Filmer, 1966; Wyman & Gill, 1990). Such a scheme with three independent gating domains is the basis of the Hodgkin–Huxley model of Na^+ channel activation (Hodgkin & Huxley, 1952). With regard to ACh receptors, stepwise gating has been briefly discussed by Colquhoun & Hawkes (1977), but has rarely been used to interpret experimental data (Colquhoun & Ogden, 1988).

Expanded versions of stepwise and concerted activation schemes are shown in Fig. 1, where the oval represents a receptor complex, and the circles and squares represent the two binding sites/gating domains present in muscle-type ACh receptors (AChR). The physical meaning of a gating domain is not specified, but each domain may span multiple subunits. For simplicity, vacant domains and monoliganded receptors are assumed not to activate. The full 3×3 matrix of states makes up the stepwise model

of activation. The outlined states (plus an added transition) constitute the concerted model of activation.

The relative complexity of stepwise and concerted models can be defined. The stepwise model for AChR has more states than the concerted model (9 *vs.* 5), but only two more rates (8 *vs.* 6). In their simplest forms, i.e. assuming either equivalent gating (stepwise) or binding (concerted) both models are of equal complexity because each has the same number of rates: association, dissociation, opening and closing. Consider a channel that has n binding sites/gating domains that each can exist in one of three states: vacant–resting, occupied–resting, or occupied–active. A stepwise gating model for such a channel will have 3^n states, while the corresponding concerted model will have only $2^n + 1$ states. For large n, the ratio of the number of states according to stepwise *vs.* concerted schemes will increase approximately as $e^{0.4n}$. For example, a receptor with five domains will have almost 10 times the number of states in the stepwise scheme as in the corresponding concerted scheme.

Model complexity is better quantified by the number of free parameters needed to determine the model (i.e. the number of rates) rather than by the number of states. For a receptor with n gating domains, the number of rates for a stepwise scheme is $4n$, while that of the corresponding concerted scheme is $2(n+1)$. Thus, in the limit of large n, the stepwise model will at most have twice as many rates as does the concerted scheme. Stepwise models are always more complex than their concerted counterparts, but always less than 2-fold.

Several simplifications have been made to arrive at the linear versions of both the concerted (model (2)) and stepwise (model (3)) kinetic schemes that were used to fit the data. For the concerted model, the two monoliganded forms are considered to be degenerate and are represented in the model by a single state, AC. For the stepwise scheme, these states as well as the two pairs of half-activated channel states have been condensed into the AC, AC*, and A_2C^* states. Also, so that concerted and stepwise models of equal complexity can be considered, I assume that the two binding sites have equal agonist association and dissociation rates. These simplifications produce the following kinetic model:

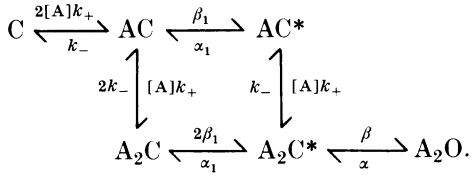

Model (4)

To arrive at the linear form of the stepwise model given by model (3), I further assume that the activation–deactivation pathway via the doubly liganded, fully unactive channel conformation (A_2C) is rare. This is valid at low agonist concentrations (where $[A]k_+ < \beta_1$), and if $\alpha_1 < k_-$. With these simplifications, the nine state, eight rate stepwise model shown in Fig. 1 is reduced to the five state, six rate scheme given by model (3) (i.e. the upper and right borders of the full model of Fig. 1). The validity of these assumptions will be considered in the Discussion.

Characteristics of AChR currents

Figure 2 summarizes the basic characteristics of the most common form of fetal-type cholinergic currents present in 60 h old *Xenopus* myocytes, and at ACh concentrations greater than ~ 2 μM. At these concentrations currents occur in bursts

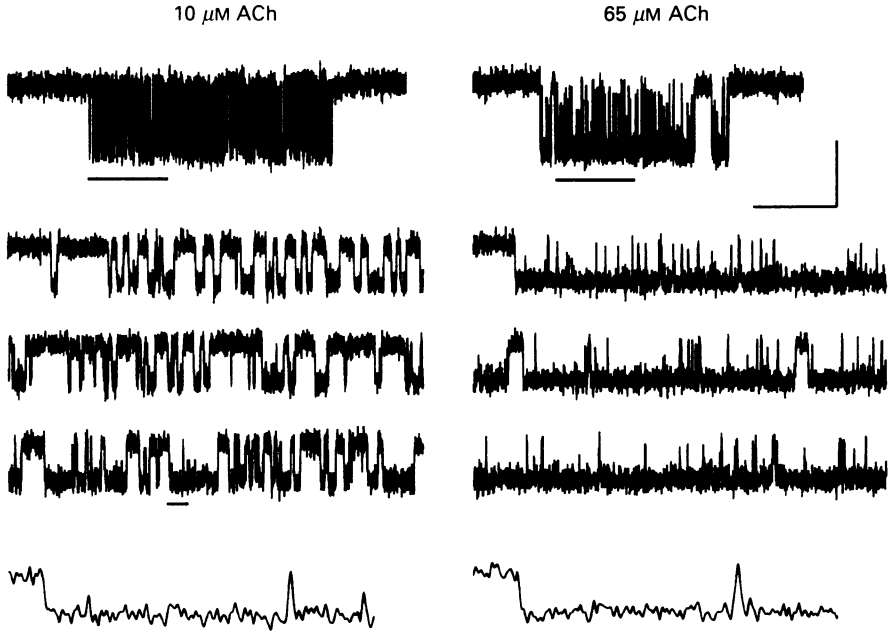

Fig. 2. Characteristics of AChR currents. Example bursts at two ACh concentrations obtained from a backfilled pipette experiment, shown at three different time resolutions. Currents occur in clusters as channels leave and enter long-lived desensitized states. Intraburst closed interval durations decrease (the effective opening rate, β', increases) as the concentration of ACh increases. Bars indicate expanded regions show below. Calibrations: upper, 625 ms, 4·7 pA; middle, 40 ms, 6·5 pA; lower, 2·3 ms, 6·5 pA (18 °C, −120 mV, analysis bandwidth = 5 kHz).

(also called clusters) that last hundreds of milliseconds as channels enter and leave the set of desensitized states (Sakmann, Patlak & Neher, 1980; Auerbach & Lingle, 1986). Within a burst, one channel moves among activatable states, and between bursts all channels in the patch are desensitized. The average intraburst closed interval duration decreases and probability of being open within a burst increases with increasing concentrations of ACh, reflecting the basic operating principle of ACh receptors: they open faster when liganded. Stated less succinctly, as the concentration of ACh increases, receptor occupancy and the frequency of channel opening increase, because the channel opening rate of doubly liganded receptors is much greater than that of vacant or monoliganded receptors.

Although intraburst closed interval durations should be described by a sum of exponential components that represents the movement of a channel through all closed states (Colquhoun & Hawkes, 1982), the distribution of both open and closed

intervals within bursts (> 0·1 ms) can each be approximated by a single exponential (Auerbach & Lingle, 1986; see Fig. 8). Because of the limited bandwidth and the specific values of the rate constants, one component of the intraburst closed interval distribution predominates above ~ 2 μM ACh, i.e. a component that can be reasonably well described by one exponential constitutes at least 70% of the detected closed intervals within bursts (Auerbach & Lingle, 1986). The characteristic rate constant of this component is called the effective opening rate, β', and reflects the rates of agonist binding and unbinding, as well as agonist-independent channel isomerization rates.

A major characteristic of muscle cell cholinergic channels is that they can be blocked by ACh (Sine & Steinbach, 1984; Ogden & Colquhoun, 1985). In my experiments (18 °C, −120 mV, 5 kHz bandwidth), the lifetime of the blocked state was usually too brief to be regularly resolved as discrete events. For unknown reasons, in a few patches channel block was more resolvable and these patches were not analysed further. At very high concentrations of ACh, blockade was manifest as a decrease in the mean and an increase in the variance of the open channel current. In these experiments, the bandwidth of the data was further limited by digital filtering (to an effective frequency of 3 kHz). In general, channel block was not a significant feature of the current interval duration distributions.

The opening rate

If binding and gating are separable, any model of activation should predict that the effective opening rate (β') will increase with increasing agonist concentrations until a limit is reached at the agonist-independent isomerization rate(s). In this section I will ignore the other components of the intraburst closed interval distributions and focus on the dependence of β' on the concentration of ACh.

The profile of the effective opening rate *vs.* the concentration of ACh in the range 2–100 μM is shown for twenty-six patches (one ACh concentration per patch) in Fig. 3. At 2 μM ACh, the mean apparent time constant of the predominant intraburst closed interval is 74·5 ms ($\beta' = 13{\cdot}4\ s^{-1}$); at 100 μM ACh, it is 0·19 ms ($\beta' = 5263\ s^{-1}$). Although there is little or no saturation in β' apparent at these agonist concentrations, some limits on β can be set by fitting the data to the Hill equation:

$$\beta' = \frac{\beta}{1 + (K/[A])^{n_H}}, \tag{2}$$

where β' is the inverse of the major intraburst closed interval time constant at ACh concentration [A], n_H is the apparent Hill coefficient (a function of the number of binding steps and co-operativity in the binding process), and K is the concentration of ACh at which $\beta' = \beta/2$ (a function of the affinity of the binding steps). The Hill equation is not useful for model discrimination as both stepwise and concerted schemes predict non-constant Hill slopes. However, it can serve as a simple starting point from which to estimate the channel opening rate, β.

Because of the lack of saturation, fitting the data with the three free parameters of the Hill equation is impossible. However, by fixing one parameter (e.g. n_H or β) and fitting the others, broad limits on the opening rate may be deduced. As the fixed

value of β is increased, the fitted value of n_H decreases (inset of Fig. 3). For example, with β set to 20000 s^{-1}, $n_H = 2{\cdot}11$ and $K = 110$ μM; with $\beta = 100000$ s^{-1}, $n_H = 1{\cdot}63$ and $K = 409$ μM. The upper and lower dashed lines in Fig. 3 correspond to β/n_H pairs of 25000/2·0 and 62000/1·7. Thus, if between 5 and 100 μM ACh n_H is less than 2, β is greater than 25000 s^{-1}.

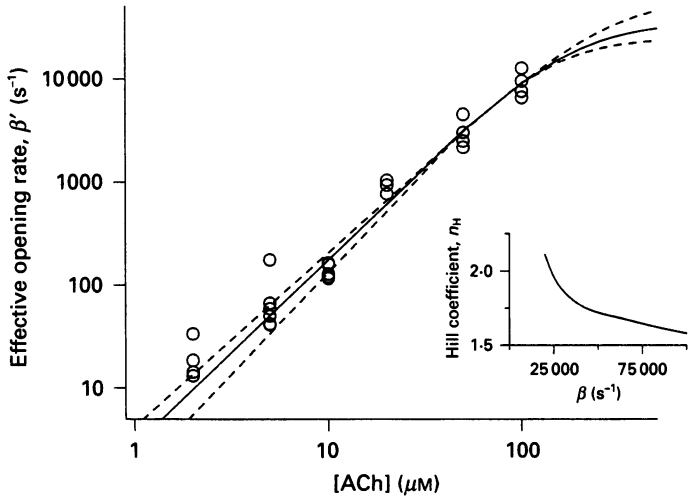

Fig. 3. The effective opening rate (β') between 2 and 100 μM ACh. Each symbol is from a different patch. The continuous line is drawn to the Hill equation (eqn (2)), with β = 30000 s^{-1} and $n_H = 1{\cdot}8$; the dashed lines are drawn with $\beta = 25000$ s^{-1}, $n_H = 2{\cdot}0$ or β = 62000 s^{-1} $n_H = 1{\cdot}7$. Over this concentration range there is little saturation in β'. Inset: relationship between the fitted values β and n_H when either is held constant. If $n_H < 2$, $\beta > 25000$ s^{-1}.

In order to gain a reasonable estimate of β it is clearly necessary to examine channel kinetics at higher ACh concentrations, i.e. > 100 μM. There are technical difficulties with these experiments. The primary problem with high-ACh experiments is that unresolved channel block increases the variance of the open channel current and interferes with the detection of resolvable closures. Lowering the system bandwidth reduces this excess variance, but also limits the detection of true closures, which are particularly short lived at high ACh concentrations. A second problem with experiments at very high ACh concentrations is that upon the approach of the patch pipette the target cell depolarizes, undergoes a massive contracture, and loads with Ca^{2+}. Although seals can be made and membranes repolarized, channel activity is often very low in these cells and the effects of Ca^{2+} loading on receptor kinetics are unknown.

I have attempted to circumvent these problems associated with high ACh concentrations, and to reduce the scatter in the β' data as well, by using backfilled patch pipettes (Auerbach, 1991). With this method target cells do not depolarize or contract because during seal formation the tip concentration of ACh is low (< 0·1 μM with a pipette backfilled with 5 mM ACh). Also, patch-to-patch heterogeneity is eliminated because multiple concentrations are examined in a single patch. In

addition, because the time dependence of diffusion in the pipette is known, the steady-state β' values can be estimated by extrapolation, i.e. information from the approach to steady state as well as the steady-state limits themselves can be used to estimate β'.

In Fig. 4, an experiment is shown where the tip of the pipette was filled with normal saline and the shank was backfilled with normal saline plus 500 μM ACh. Example bursts and closed interval duration distributions are shown as a function of time after backfilling. The gating time constants, obtained by fitting closed interval distributions to one exponential, diminish with time, from ~ 350 μs 3 min after backfilling to ~ 75 μs about 10 min after filling, because of the increasing concentration of ACh.

Although diffusion in a cone as a function of time is computed as an infinite sum of exponentials, at sufficiently long times after backfilling, the concentration of ACh at the tip increases as a single exponential (eqn (1)). As a first approximation, a linear relationship between β' and the ACh concentration was assumed, and the $1/\beta'$ *vs.* time data was fitted to an exponential plus a constant that reflects the steady-state β' value at the shank concentration of ACh.

To test the validity of this method, extrapolated β' values from backfilled patch experiments (10, 20, 50 and 100 μM ACh) were compared with those from single-concentration patches. There was a good agreement between the values obtained by both methods, i.e. in each patch the extrapolated value was in the range of those obtained with single-concentration patches.

For the patch shown in Fig. 4, the fitted constant was $0{\cdot}053 \pm 0{\cdot}022$ ms (90% confidence limit), corresponding to a β' value at 500 μM of ~ 18870 s^{-1}. Note that the error limits on this value are very large and should be even larger: the offset value strongly depends on the durations of closed intervals from bursts at high ACh concentrations, and these are the fewest, fastest and least accurately measured gaps. Also shown in Fig. 4 are similar data from two pipettes backfilled with 200 and 5000 μM ACh. The extrapolated steady-state β' values for these experiments were 7890 s^{-1} and 25000 s^{-1}. In the upper panel, the frequency of gaps (per unit open time) is shown for the 200 μM ACh patch. That this parameter did not vary over the course of the experiment indicates that gaps arising from channel blockade by ACh did not substantially contaminate the record.

Figure 5 shows that extrapolated β' values for ACh concentrations between 100 and 5000 μM (twelve patches). A fit to the Hill equation (eqn (2)) over this concentration range produced an estimated saturation at $\sim 24870 \pm 1125$ s^{-1}.

Single-patch dose–response curves

In backfilled patch experiments, estimates of β and n_H may be gained by transforming time into dose according to eqn (1), thus allowing β' to be plotted as a function of the ACh concentration in a single patch. This transformation essentially produces a single patch version of the dose–response curves shown in Figs 3 and 5. The advantage of this approach is that the assumptions of an exponential increase in ACh concentration and a linear relationship between concentration and β' are avoided, and that scatter in the β' *vs.* ACh curve arising from patch-to-patch heterogeneity is eliminated. The disadvantage of this method is that the transform

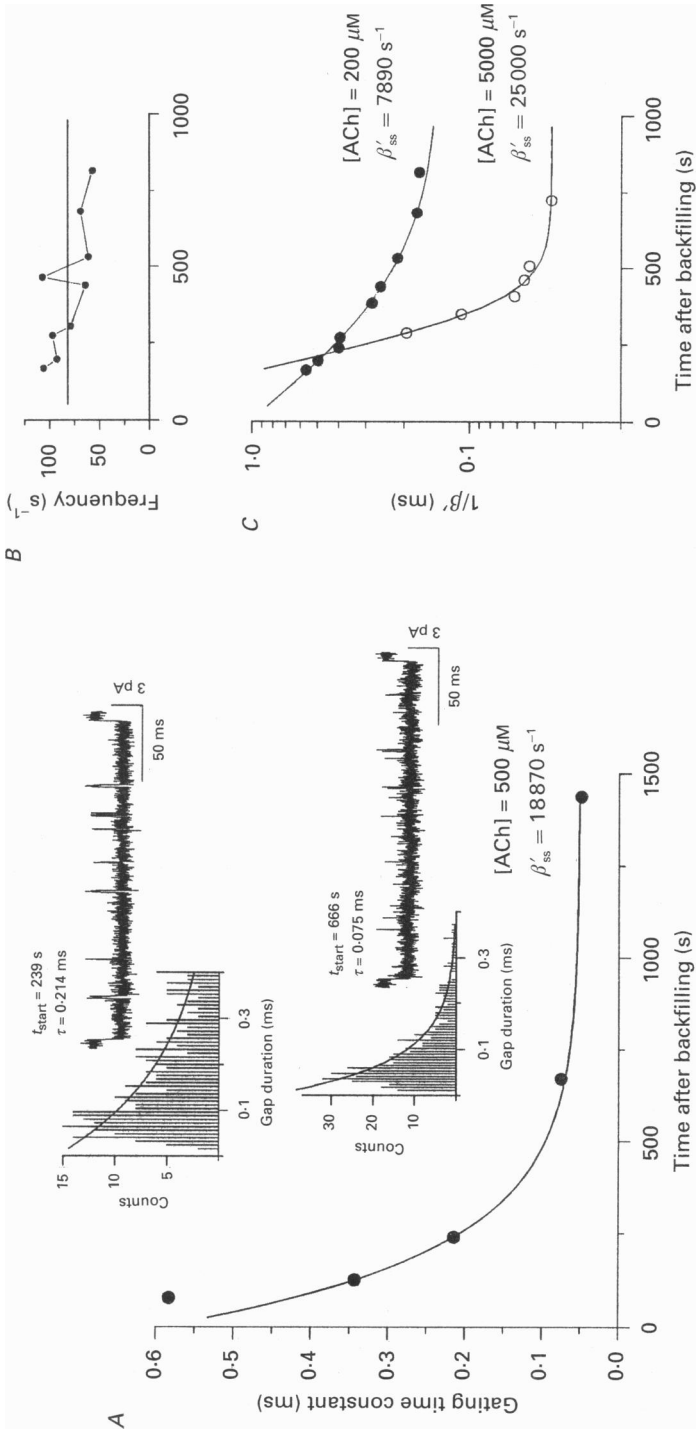

Fig. 4. Estimating β' from backfilled pipette experiments. *A*, the points are from a single patch and represent the time constant of the main intraburst closed interval component ($1/\beta'$) measured from histograms compiled at different times after backfilling. The line is a fit (first point excluded) to an exponential plus a constant. The reciprocal of the fitted constant, β'_{ss}, is the steady-state effective opening rate at the shank ACh concentration. Example histograms and current bursts are shown as insets, where t_{start} is the time after backfilling that the burst began, and τ is the fitted time constant of the histogram. In this patch the shank concentration of ACh was 500 μM and $\beta'_{ss} = 18820\ s^{-1}$. *C*, Analyses of two other backfilled patch experiments at shank ACh concentrations of 200 and 500 μM. *B*, the frequency of intraburst gaps per unit open time (200 μM experiment). Gaps arising from channel block, which should be more prevalent at higher ACh concentrations, are absent. The gap frequency appears to decrease with concentration because gaps get shorter, thus more escape detection.

depends on an accurate knowledge of both the fill height and the ACh diffusion constant. Thus the computed dose–response profiles are subject to greater errors than a simple fit to the time-dependent data.

Two examples of single patch β' time– and dose–response curves are shown in Fig. 6. As with single-concentration experiments, the β' values from the experiment

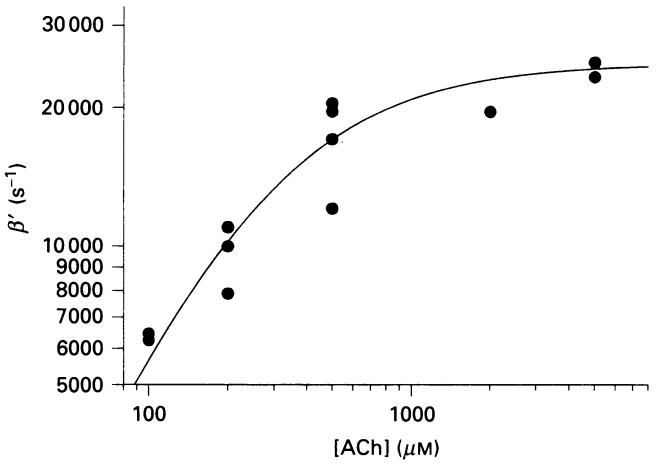

Fig. 5. The effective opening rate estimated from backfilled pipettes at very high ACh concentrations. Each point is the steady-state β' value from a backfilled patch experiment (see Fig. 3). The continuous curve is drawn to a Hill equation with $\beta = 24870\ s^{-1}$, $n = 1{\cdot}4$.

with a pipette backfilled with 100 μM ACh did not show any apparent saturation. With n_H fixed to 1·8, fitting these data to the Hill equation produced a β estimate of 23003 s^{-1}. The β' values from the pipette backfilled with 5 mM ACh did indeed saturate, and the channel opening rate could be independently estimated from a fit to the Hill equation ($\beta = 22260 \pm 1617\ s^{-1}$).

The conclusion of this analysis of the concentration dependence of the effective opening rate is that once doubly liganded, *Xenopus* myocyte fetal cholinergic receptors open rapidly at a rate $> 25000\ s^{-1}$. It is important to emphasize that this rate is close to the time resolution of the system, and thus must be considered to be a lower limit on the opening rate, β. In the following section, single-channel current kinetics are analysed with respect to both the concerted, model (2), and stepwise, model (3), activation schemes.

Burst kinetic analysis – an example patch

Rate constants were estimated by the method of Horn & Lange (1983), with the first-order approximation of Roux & Sauve (1983) incorporated to correct for the effects of limited bandwidth. The likelihood of observing sequences of intraburst open–closed interval durations for a given model were computed, and the rates of the model were iteratively adjusted until this likelihood was maximal.

An example analysis is illustrated in Figs 7–10 for a cell-attached patch where the

pipette contained 5 μM ACh. In this patch twenty-five bursts (τ_c = 100 ms) were selected for analysis based on the following criteria: at least five open intervals, a mean open interval duration > 1 ms, and a mean open interval amplitude between 3·5 and 4 pA (to exclude currents from the larger amplitude adult-type cholinergic

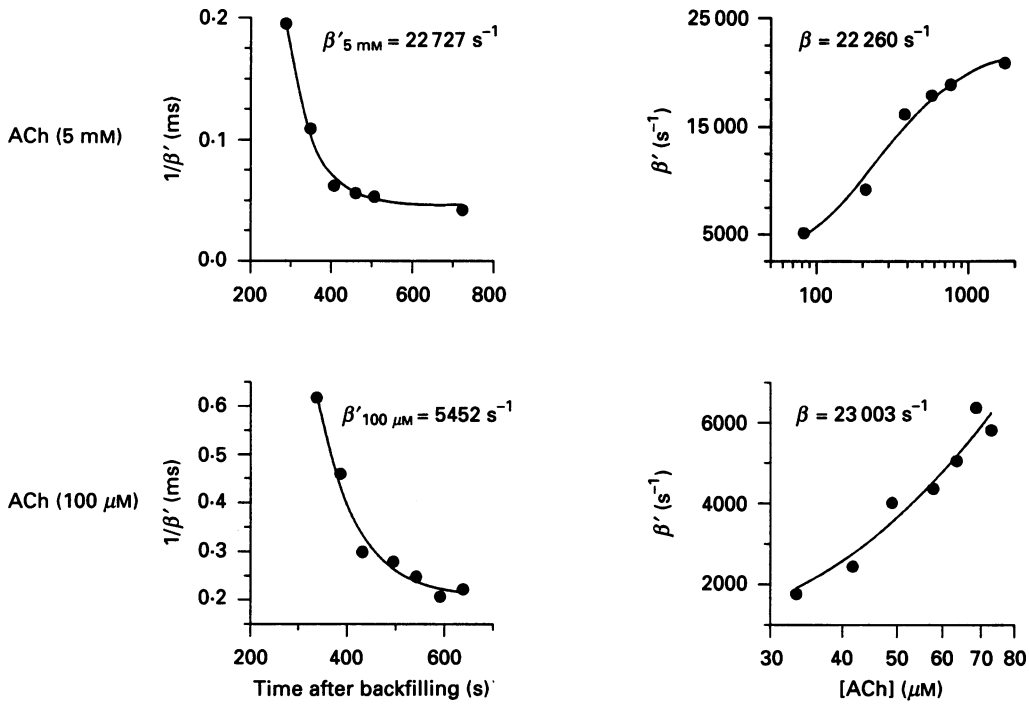

Fig. 6. Single-patch dose–response curves of the effective opening rate. The results from two patches are shown (the shank concentration of ACh is indicated at the left). Time constants obtained from fitting intraburst closed interval duration histograms are plotted both as a function of time after backfilling, or as a function of the tip concentration, computed according to eqn (1). The dose–response curves are single-patch versions of the data shown in Fig. 3.

channel). The purpose of the selection process is to minimize the contribution of heterogeneous channels. On average, the twenty-five bursts that were selected were 844 ms in duration, contained sixty-six open intervals, had a probability of being open (P_o) of 0·15, and were made up of open and closed interval durations that had means of 2·14 and 16·4 ms, respectively.

The interval durations within the selected bursts were fitted to both the concerted and stepwise activation models, with varying degrees of constraint imposed on the kinetic parameters. In all cases, the channel opening rate β was fixed to be 30000 s^{-1}. This was necessary because there is little information at any single agonist concentration about the value of β. This constraint also added stability to the missed event correction. Errors introduced by fixing the opening rate value will be considered in a later section.

The effects of limited bandwidth can be seen in Fig. 7, which shows a histogram of open interval durations. The continuous curve was computed from the fitted rates (stepwise model) with a correction for missed events; the dashed curve is that predicted from the rates assuming infinite bandwidth. For all models, the estimated

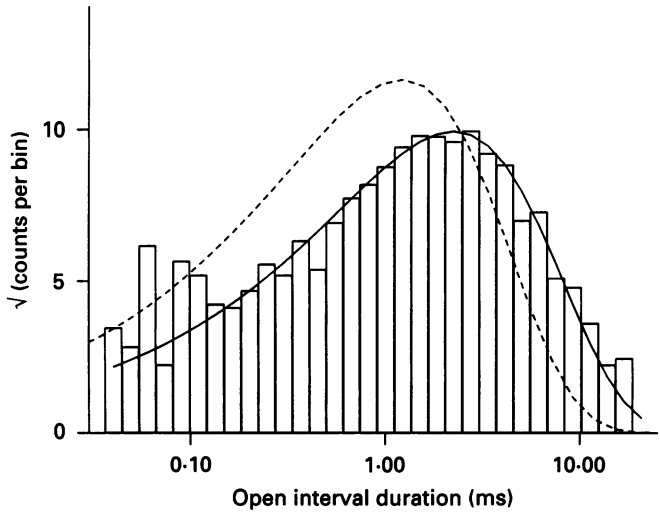

Fig. 7. Open interval duration histogram. The lines were computed from the rate constants obtained by maximum-likelihood fitting according to the stepwise model (partial symmetry; see Fig. 9 for companion closed interval duration histogram). Under experimental conditions, short-lived closures that escape detection cause the apparent open channel lifetime at an analysis bandwidth of 5 kHz (continuous line) to be greater than that predicted from the rates assuming infinite bandwidth (dashed line).

closing rate, α, was $\sim 750\ s^{-1}$ (dashed curve). This is almost twice the apparent closing rate computed from the mean open time ($400\ s^{-1}$; continuous curve) because many brief closures were not detected by the threshold-crossing algorithm.

Closed interval duration distributions, too, are altered by filtering. Whereas the effect of limited time resolution on open intervals is to increase the duration of the predominant component, its major effect on the closed interval probability density function (pdf) is to reduce or eliminate the relative contribution of fast gaps.

Three parameter fit

In their simplest forms and with β fixed, both the concerted and stepwise models require only three parameters to be fitted: an association rate, a dissociation rate and a closing rate. With the concerted model, this assumes equal and independent binding to both sites ($k_{+1} = 2\,k_{+2}$ and $k_{-2} = 2\,k_{-1}$); with the stepwise model, this assumes equal and independent isomerization rates for both subunits ($\alpha = 2\alpha_1$ and $\beta_1 = \beta$). Colquhoun & Ogden (1988) have fitted burst P_o *vs.* ACh profiles to this version of the stepwise activation model.

The fits to the single channel interval durations of the example data file assuming these fully symmetric (equivalent binding or gating) versions of the models are

shown in Fig. 8, where the computed closed interval distributions are superimposed on a histogram of interval durations. The likelihood profiles for each of the fitted rates, too, are shown to the right; the log likelihood (LL) and likelihood ratio (LLR) values are also shown and are given in Table 1A along with the rate estimates.

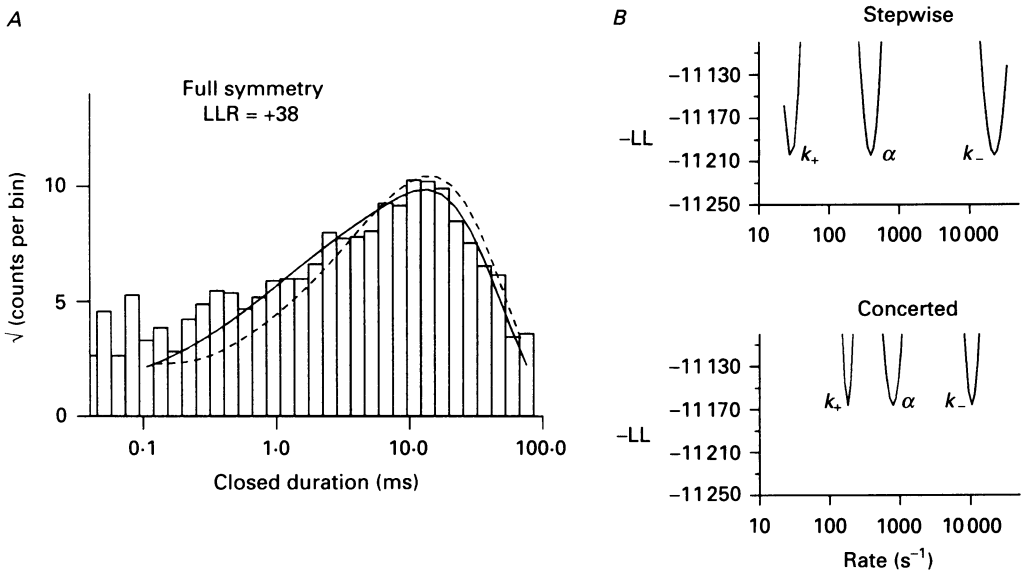

Fig. 8. Closed interval duration histogram, full symmetry (equal binding with the concerted model or equal gating with the stepwise model; three free parameters). *A*, histogram compiled from interburst closed intervals; the lines were computed from the model parameters obtained by fitting the discrete interval data and are *not* a fit to the binned data. The stepwise model (continuous line, log likelihood (LL) = 11 204) produced a higher log likelihood than the concerted model (dashed line, LL = 11 166), as indicated by the positive log likelihood ratio (LLR). *B*, the LL profile plotted for different rate values (other rates held at their optimum values). The lower −LL of the stepwise model compared to the concerted model indicates a superior fit; the broader LL profiles for some rates indicates a larger standard error (see Table 1 for the rate estimates, and Figs 14 and 15 for a description of standard errors of the rate estimates).

The fit to the data at 5 μM according to the symmetric concerted model is reasonable and would not be rejected out of hand. The predominant closed interval component is fairly well described by the fitted parameters (τ = 13·2 ms; 94% of all gaps); only small component of closures ~ 0·5 ms is not well accounted for by the rates. Sine *et al.* (1990) have noted the significance of these intermediate duration gaps: according to the concerted model they reflect the different binding affinities of the two sites. Cruder indices of the adequacy of the fit, such as the general appearance of currents simulated according to the model parameters and the computed probability of being open at 5 μM ACh (0·194), also do not cause an immediate rejection of the model at this single concentration. According to the fit to the concerted scheme, the rate of binding to a single site is $1{\cdot}8 \times 10^8$ s^{-1} M^{-1} and the computed single-site affinity is 57 μM. A fast (79 μs) gap component which would

have constituted 68% of the total at infinite bandwidth is virtually absent (2·5% of the total) at 5 kHz.

The fit to the symmetric form of the stepwise model assumes each gating domain acts identically to and independently of its companion. This model (continuous line) fits the data better than in the concerted model (LLR = +38) even though the same number of parameters were required. In addition to describing the major component of closed intervals (83% at 14·8 ms), the computed closed interval distribution now predicts an intermediate component (13% of the gaps from a component with $\tau = 2{\cdot}1$ ms), therefore producing the higher likelihood value than with the similarly constrained version of the concerted model. The predicted single-site affinity was a surprisingly high 494 μM, with a fast dissociation rate of 22247 s^{-1}.

According to the stepwise scheme, the low intrinsic affinity for agonist is counterbalanced by a high activation/deactivation ratio (76) that serves to 'trap' the ligand in its site (since agonist cannot escape from an active domain) and increase the effective opening rate at low agonist concentrations. If agonist cannot escape from an active domain, the effective dissociation rate (k_-^*) will be reduced relative to the actual value (k_-):

$$k_-^* = \frac{k_-}{1 + (\beta_1/\alpha_1)} \tag{3}$$

Because the lifetime of a liganded subunit is about 75 times longer than that of the liganded-unactive subunit, the effective dissociation constant is reduced to 6·5 μM from its actual value of ~ 500 μM. Thus, as a consequence of agonist 'trapping', the effective opening rate is high even at ACh concentrations well below the actual dissociation constant (K_d). Note that Auerbach & Lingle (1987) have reported a half-maximal P_o for fetal-type channels of ~ 5 μM.

If the activation–deactivation isomerization is not explicit to the model (e.g. if data from the stepwise process is interpreted according to a concerted model), there will be an apparent negative co-operativity to activation, with the first ligand to bind appearing to have a higher affinity (here, 76-fold) for the channel than does the second. With the fully symmetric version of the stepwise model, each gating domain remains in the active conformation for about 2·8 ms before deactivating, or just twice as long as in the open channel lifetime (recall that the apparent open channel lifetime is longer than true time value because of missed events).

Four-parameter fit

To test the assumptions of independent and identical binding/gating the constraints were relaxed in a graded fashion. With the concerted model, the association rates were held equivalent ($k_{+1} = 2\ k_{+2}$) but the dissociation rates were allowed to vary between sites. With the stepwise model, the constraint of equivalent domain deactivation rates was relaxed but the subunit activation rate was assumed to be invariant ($\beta_1 = \beta$). In these partially symmetric versions of the model there are four free parameters. The results are shown in Table 1B and in Fig. 9.

With the concerted model, allowing partial asymmetry in binding improved the fit relative to the fully symmetric form of the model (LLR = +42 with one additional free parameter). The estimated rate of dissociation from the second site was ~ 10

times that of the first, resulting in single-site equilibrium affinities of 155 and 15·6 μM. The computed closed interval distribution fitted the intermediate component of gaps (6% at 0·53 ms) better than the fully symmetric version.

In the stepwise model, partial symmetry means that a gating domain's deactivation rate is allowed to differ and/or depend on the conformation of its

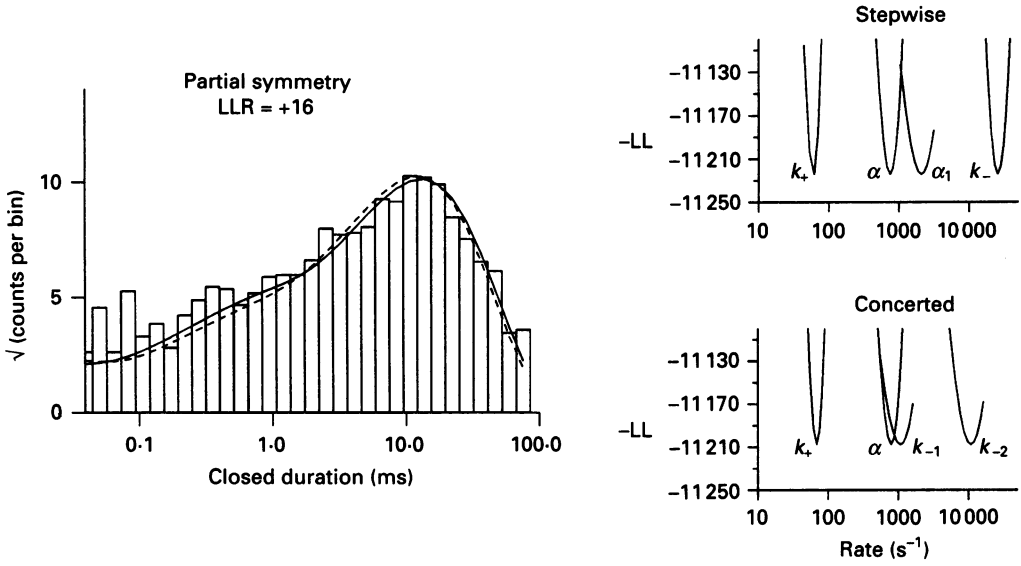

Fig. 9. Closed interval duration histogram, partial symmetry (equal association with the concerted model or equal activation with the stepwise model; four free parameters). The binned data and curves were obtained as described in Fig. 8. The positive LLR indicates that the stepwise model (continuous line, LL = 11 224) provided a better fit to the data than the concerted model (dashed line, LL = 11 208) (see the lower left panel of Fig. 17 for the LLR distribution obtained by resampling). With both models, the −LL values are lower than those from fits with only three free parameters, indicating that activation is asymmetric.

counterpart. As with the concerted model, the fit to this version of the model significantly increased the likelihood of the fit (LLR = +20, one additional parameter). The partially symmetric version of the stepwise model predicts that the domain deactivation rate decreases about 5·5-fold when the channel is in the conducting conformation, i.e. the active conformation is stabilized in the open channel. Accordingly, the ratio of activation/deactivation rates increases from about 14 to 80 between non-conducting and conducting channels. A major difference compared to the fully constrained version of the model is a decrease in the predicted equilibrium dissociation constant to 273 μM, because of an increase in the association rate to $\sim 0{\cdot}9 \times 10^8$ s^{-1} M^{-1}. With regard to the intermediate duration gaps, the rates predict that about 10% of closures belong to a component which has a characteristic time constant of 0·63 ms, much faster than with the fully constrained stepwise model. The open interval distribution, too was also better described by this version of the model (not shown).

Five-parameter fit

Finally, both binding rates of the concerted model, and the gating rates of the stepwise model, were allowed to be non-equivalent (Fig. 10). Each fit had five free parameters. With the concerted model, the fit again improved relative to the

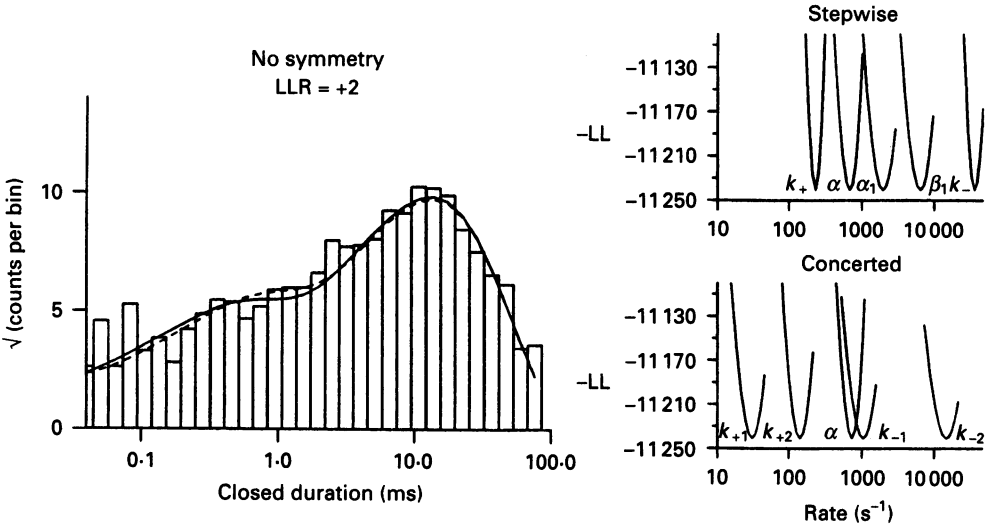

Fig. 10. Closed interval duration histogram, no constraints on the equivalence of binding or gating rates (five free parameters). The binned data and curves were obtained as described in Fig. 8. The stepwise model provided the better fit. Concerted model: dashed line, LL = 11240. Stepwise model: continuous line, LL = 11242.

partially symmetric version (LLR = +32, with one additional parameter). The computed closed interval distribution fitted the intermediate gap component better than that which was computed with the assumption of equivalent association rates, with 17% of gaps predicted to belong a component with a mean lifetime of 0·61 ms. The dissociation from the second site is still 10 times faster than from the first, but in this version of the model the association rate is also increased at the second site by about 4-fold, with the net result being a K_d of 34·8 and 102 μM at the two sites.

Fully relaxing the constraints of equivalence with the stepwise model also improved the fit (LLR = +18, one additional parameter). The estimated opening rate of the first gating domain to isomerize, β_1, was 7868 s^{-1}, or about 4 times slower than the channel opening rate. The single-domain deactivation rate α_1, remained $\sim$ 5 times faster than $\alpha/2$. Thus, according to the rates activation is speeded and deactivation slowed when the counterpart domain is in the activated conformation. The single-site K_d was 201 μM.

The results of fitting the example data file can be summarized as follows. All three versions of both models provide reasonably good descriptions of the data. For both the concerted and stepwise models, the freedom from equivalence in binding

(concerted) or gating (stepwise) improved the fit, i.e. the activation process is asymmetric. The likelihood of the stepwise model is greater than that of the concerted model under all symmetry constraints.

Other patches

A total of nine files in the concentration range 2–100 μM ACh have been analysed in the same manner as the above example, with the single subunit activation rate fixed at 30000 s^{-1}. The results of fitting these patches under the conditions of full, partial, or no symmetry are summarized in Table 1. Among these data are results from three experiments with backfilled pipettes.

For both models, allowing asymmetry in the gating process increased the likelihood of the fit. This was true not only for the aggregate likelihood from all patches, but also for every individual patch save one. This increase is not simply due to the addition of an extra free parameter as the symmetry constraints were relaxed. Overall, the asymptotic information criteria (AIC; Horn, 1987) were positive in the comparison of partial-to-full symmetry (+293 for concerted, +361 for stepwise) or none-to-partial symmetry (+205 for concerted, +161 for stepwise) versions of both models. The largest increase in likelihood was realized when dissociation rates were allowed to vary at the two binding sites ($k_{-2} \neq 2\ k_{-1}$; concerted model), or when the subunit inactivation rate was allowed to vary depending on the isomerization status of the other subunit ($\alpha \neq 2\ \alpha_1$; stepwise model). These results clearly indicate that activation of AChR is an asymmetric process.

For a given degree of constraint, concerted and stepwise models can be directly compared by the likelihood values because each model has the same number of free parameters. A positive value in the last column of Table 1 indicates that the stepwise model provided the superior fit, and a negative number indicates that the concerted model provided the better fit.

Under the assumption of full symmetry (Table 1 A), in five of nine files the stepwise model fitted better. The aggregate log likelihood, too, was greater for the stepwise model (LLR = +12). With partial symmetry (Table 1 B), the stepwise model again better described the data. For the bigger data files (more than 2500 intervals) all were better fitted by the stepwise scheme. For the smaller data files, four of five were better described by the stepwise scheme. The aggregate fit to the stepwise model was better than that of the concerted model (LLR = +46). Finally, the models can be compared without assumptions of symmetry, where each model had five parameters to be estimated (Table 1C). Of the larger data files, three of four were better fitted by the stepwise model; the other was equally described by both models. Of the smaller files, two were better fitted by the concerted model, two by the stepwise model, and one produced identical log likelihoods. For the aggregate, the likelihood of the stepwise version was greater than that of the concerted scheme (LLR = +24). The significance of the LLR values, and the standard error estimates on the fitted parameters, are discussed in a later section.

Overall, the stepwise scheme provides a better description of gating than does the concerted scheme, as judged both by a file-by-file comparison, or by the aggregate likelihood estimates. For each file, the same number intervals were subjected to the same optimization procedure. In twenty-seven pairwise comparisons of the two

TABLE 1. Summary of results of fitting nine files under conditions of full, partial or no symmetry

A. Full symmetry (three free parameters)

			Concerted				Stepwise				
File	n	ACh	k_+	k_-	α	LL	k_+	k_-	α	LL	LLR
703226	79	100	208	8342	741	37483	187	13673	768	37486	+3
681580	35	10	431	7131	594	19484	79	14695	593	19488	+4
390001	25	5	183	10475	795	11166	45	22247	791	11204	+38
322674	38	10	146	10495	613	11874	31	19231	625	11856	−18
713540	47	5000	90	11990	615	4749	75	26863	588	4756	+7
320825	21	10	137	4942	355	2226	17	9278	361	2220	−6
321709	16	10	55	4827	799	2140	26	31945	490	2122	−18
366840	12	5	222	5866	500	1850	210	51108	297	1854	+4
330689	13	2	133	4723	459	1142	25	10497	468	1140	−2
Sum						92114				92126	+12
Mean			155	7643	608		77	22170	553		
S.D.			115	2640	144		68	12440	157		

B. Partial Symmetry (four free parameters)

			Concerted					Stepwise					
File	n	ACh	k_{+1}	k_{-1}	k_{-2}	α	LL	k_+	k_-	α_1	α_2	LL	LLR
703226	79	100	138	1870	16734	736	37534	161	17417	4755	705	37537	+3
681580	35	10	190	1425	11396	560	19503	153	17830	3557	567	19514	+11
390001	25	5	69	1071	21626	787	11208	87	25365	2078	745	11224	+16
322674	38	10	72	1794	22480	603	11894	100	27289	3668	571	11905	+11
713540	47	5000	73	2353	23974	581	4753	89	24787	3247	614	4757	+4
320825	21	10	110	2916	10137	353	2226	65	10506	10716	350	2227	+1
321709	16	10	28	1011	9227	807	2142	64	34317	2928	473	2136	−6
366840	12	5	150	1907	15485	452	1853	309	49621	2841	295	1857	+4
330689	13	2	68	1087	10476	453	1148	78	9922	4846	468	1150	+2
Sum							92261					92307	+46
Mean			100	1715	15726	592		123	24117	3865	532		
S.D.			48	606	5470	150		74	11727	2630	142		

C. No Symmetry (five free parameters)

			Concerted						Stepwise					
File	n	ACh	k_{+1}	k_{-1}	k_{+2}	k_{-2}	α	LL	k_+	k_-	β_1	α_1	α	LL	LLR
703226	79	100	190	1364	145	17881	727	37536	304	27498	16124	5600	664	37556	+20
681580	35	10	183	260	163	7748	654	19521	246	22056	11562	3168	539	19523	+2
390001	25	5	61	1045	143	29283	727	11240	231	46389	7868	1674	645	11242	+2
322674	38	10	77	2068	147	31968	547	11911	151	33101	12553	2825	543	11911	0
713540	47	5000	171	3480	91	35922	544	4753	149	22348	8812	3252	697	4768	+15
320825	21	10	139	4590	248	11504	346	2228	109	11354	6104	5697	344	2228	0
321709	16	10	34	4857	453	69601	409	2148	192	37989	5878	4939	466	2143	−5
366840	12	5	130	2012	328	21973	400	1861	583	57029	7568	2291	583	1862	+1
330689	13	2	31	2890	948	19925	408	1116	107	10448	5397	1390	481	1155	−11
Sum								92364						92388	+24
Mean			112	2507	296	27311	529		230	29801	9096	3426	551		
S.D.			60	1486	254	17297	139		139	14644	3405	1532	105		

The rates are s^{-1}, except k_{+1} and k_{+2} which are $s^{-1}\,\mu M^{-1}$; ACh is μM; n is the number of bursts that were analysed. Files 703226. 681580. and 713540 were backfilled with the indicated concentration of ACh.

models, eighteen favoured the stepwise form, seven favoured the concerted form, and two produced identical likelihood estimates.

Xenopus cholinergic channels change their kinetic properties dramatically during development, and computing averages across files that may be heterogeneous is ill advised. Nonetheless, the average rates given in Table 1C indicate that according to the fully asymmetric version of stepwise scheme, ACh binds at each site at a rate of $2{\cdot}3 \times 10^8$ s^{-1} M^{-1} and dissociates at a rate of 29800 s^{-1}, with an equilibrium dissociation constant of 130 μM. The gating rates of each domain are different and/or are influenced by the conformational status of its counterpart. Once liganded, an unactive domain activates at a rate of 9100 s^{-1} or 30000 s^{-1}. Once activated, a domain will deactivate at a rate of 3400 s^{-1} or 225 s^{-1}.

Backfilled pipettes

Both the necessity of constraining parameters and the high degree of variability in the fitted rates is in part attributable to the lack of information in the data from any single concentration. Fitting many different patches, each taken at a different ACh concentration, as a whole may restrict the shape of the likelihood function and produce a better fit. Heterogeneity in channel kinetics, however, reduces the utility of such an aggregate fit.

To reduce this source of error, but still obtain fits over a range of agonist concentrations, intraburst channel currents from backfilled pipettes were analysed. For each burst the concentration of ACh was computed from its starting time (eqn (1)) and the product of this value and the association rates were entered into the transition matrix. Three patches were fitted in this manner.

The filled symbols in Fig. 11 show an experiment where a pipette was backfilled with 100 μM ACh. The diffusion time constant for this patch was 517 s (fill height = 1·75 mm); the seventy-nine bursts that were analysed started from 278 to 888 s after dislodging the bubble that separated tip and shank solutions. These times correspond to ACh concentrations of 4·9–64·3 μM.

The rate estimates and likelihood values for this file were fitted according to the concerted and stepwise models and are shown in Table 1. Without the constraints of symmetry, the concerted model predicts an association rate of about $1{\cdot}9 \times 10^8$ s^{-1} M^{-1} to each site, but, as with the single-concentration patches, about a 10-fold faster dissociation from one site than the other (1360 and 17900 s^{-1}). The stepwise model predicts a somewhat faster association rate of $3{\cdot}0 \times 10^8$ s^{-1} M^{-1}, and a dissociation rate of 27500 s^{-1}. The computed single-site equilibrium dissociation constants are 90 μM (stepwise), and 14 and 62 μM (concerted). According to the stepwise model, the deactivation rate of one domain is $\sim$ 17 times faster (5600 s^{-1}) than in that of the other channel (332 s^{-1}), and the single-domain activation rates of the two domains differ by about a factor of two.

The mean intraburst closed interval durations from two other pipettes backfilled with either 10 μM (analysis range: 5·2–9·7 μM) or 5000 μM (analysis range: 55–649 μM) ACh are also shown in Fig. 11, and the rate estimates are given in Table 1. The similarity of the association rate with these patches compared to single-concentration patches indicates that the concentration normalization procedure is accurate.

Predictions of the fitted parameters

It is useful to discuss the predictions of the stepwise activation model with regard to channel currents at limiting high and low agonist concentrations for both forms of model. The concerted model has been thoroughly covered by Colquhoun &

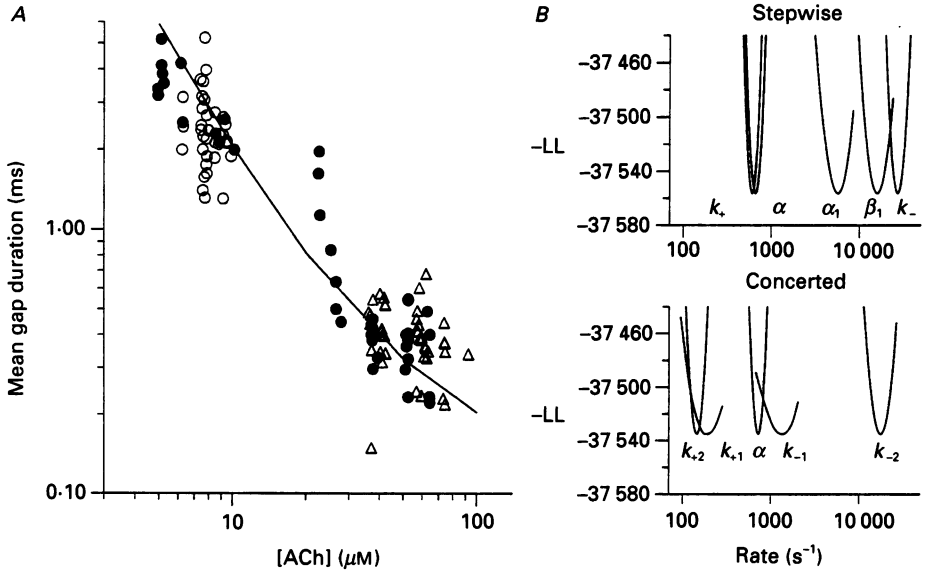

Fig. 11. Maximum-likelihood analysis of backfilled pipette experiments. *A*, the mean intraburst gap durations are plotted as a function of the computed ACh concentration (each point is a burst) for three backfilled pipette experiments (shank ACh concentrations: △, 5 mM; ○, 10 μM; ●, 100 μM). Interval durations from each burst were fitted by a maximum-likelihood procedure after scaling the association rate(s) of the model by the computed concentration. The continuous line is the predicted gap duration obtained from the rates of the stepwise model (100 μM experiment) with no constraints for activation symmetry. *B*, likelihood profiles of the rates for the 100 μM ACh experiment (five parameters); the stepwise model provided the better fit to the data. (LL = 37556 *vs.* 37536 for concerted model).

Hawkes (1977) and predicts that closed intervals within bursts should have durations that are distributed as a single exponential with a characteristic time constant of τ_{gap} (two-state, closed–open system) both at very high concentrations, where $\tau_{gap} = 1/\beta$, and at very low concentrations, where $\tau_{gap} = 1/(\beta + k_{-2})$.

Because there are three species of doubly liganded channel in the stepwise activation model (with zero, one, or two subunits activated), at the concentration extremes the model reduces to a three-state scheme (doubly-liganded states only):

$$\begin{array}{ccccc} & k_{-1}\uparrow & & k_{-1}\uparrow & \\ & & 2\beta_1 & & \beta \\ A_2C & \rightleftharpoons & A_2C' & \rightleftharpoons & A_2O. \\ & & \alpha_1 & & \alpha \end{array} \qquad \text{Model (5)}$$

At very high agonist concentrations the effective association rate becomes infinite

and the dissociation rates may be ignored in the computation of gap durations. At limiting high and low agonist concentrations closed intervals should be described by the sum of two exponentials.

At very low agonist concentrations, according to the stepwise model at infinite bandwidth with $\beta = 30000\ s^{-1}$, $\beta_1 = 9100\ s^{-1}$, $\alpha_1 = 3400\ s^{-1}$ and $k_- = 28900\ s^{-1}$, 87% of gaps within bursts should belong to an exponentially distributed component with a time constant of 17 μs with the remainder from a component with a time constant of 13 μs. These are experimentally inseparable, and in an analysis of low concentration gaps, corrected for bandwidth, they would appear as 16 μs gaps at a frequency of 0·95 per burst. According to the concerted model with $\beta = 30000\ s^{-1}$ and $k_{-2} = 27000\ s^{-1}$, a single gap component with a duration of 18 μs should occur at a frequency of 1·1 per burst. The stepwise and concerted schemes cannot be distinguished by gap properties at limiting low ACh concentrations.

At saturating high concentrations, the stepwise model predicts that gap durations should also be distributed as the sum of two exponentials. With a τ_m (dead time) of 35 μs, 50% should be from a component with a characteristic time constant of 68 μs with the other half from a component with a characteristic time constant of 28 μs. Given the bandwidth and sampling limitations, it is impossible to resolve these two components, which should fuse to form a single component with a time constant of about 48 μs, or an apparent maximum β' of $20833\ s^{-1}$. According to the stepwise model, the saturation value of β' is always less than the true channel opening rate. Of course, the concerted model predicts the β' values to saturate at β, i.e. at $30000\ s^{-1}$. Bandwidth and sampling limitations also frustrate a distinction between stepwise and concerted models at limiting high ACh concentrations.

The predictions of the stepwise model are shown in Fig. 12. Between 2 and 100 μM ACh, there is reasonably good agreement between the experimentally observed β' values and those predicted from the rate constants of the stepwise model without constraints of symmetry. These data indicate that burst P_o, too, would be well described by the asymmetric version of the stepwise scheme.

Although closed intervals within bursts at a concentration 2 μM would appear to be distributed as a single exponential, according to the stepwise scheme these gaps would be derived from two separate components that together constitute 90% of closures at all ACh concentrations. At lower ACh concentrations, the intraburst gaps are predominantly from the slower (λ_1) component, and at high ACh concentrations they are derived from the faster (λ_2) component. The cross-over concentration is about 80 μM, where at a bandwidth of 5 kHz, about half of the gaps would arise from a component with a time constant of 0·28 ms and about half with a time constant of 0·08 ms, producing what would appear as a single exponential with a time constant of 0·18 ms ($\beta' = 5500\ s^{-1}$). Above this concentration, the slower component becomes separable on the basis of time constant but contributes too few gaps to be detected. Below $\sim$ 80 μM, the faster component makes too small a contribution to be detected. Thus, to a first approximation, gaps would appear to be distributed as a single exponential at all ACh concentrations. According to the average rates of the stepwise model, the intermediate gaps that are present in Figs 8–10 (5 μM ACh) are the faster component that is just barely separable (12% at $\tau = 0{\cdot}3$ ms) from the major, slower component (78% at $\tau = 12{\cdot}5$ ms).

Errors in the rate estimates

It is important to set error limits on the rates given in Table 1. I will consider two sources of inaccuracy: from biases inherent to the analysis, and from the standard errors of the parameters.

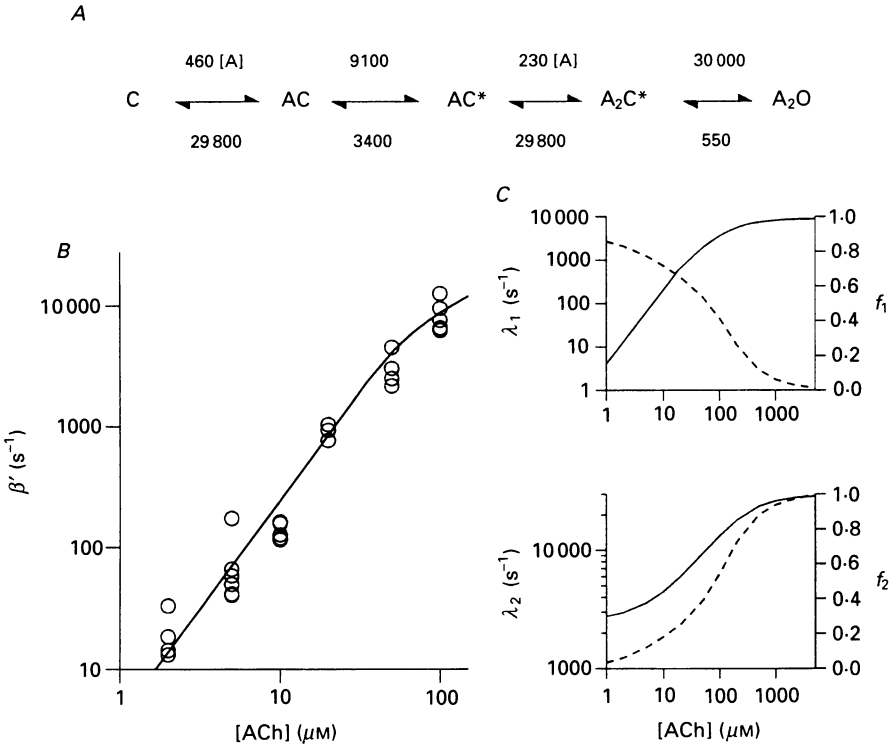

Fig. 12. Predictions of the stepwise model. *A*, the average rates from nine experiments, according to the stepwise activation scheme (five free parameters; see Table 1C). The rates are s^{-1}, except for k_+ which is μM^{-1} s^{-1}. *B*, the effective opening rates from single-concentration patches (symbols; see Fig. 3) and those computed from the rates of the model are shown as a function of the ACh concentration. The predicted and experimental values are in good agreement. *C*, the eigenvalues (λ) and fractional contributions (f; dashed line) of the two predominant components of the closed interval distribution that are predicted by the rates of stepwise model. The apparent β' values shown in *B* were computed as $\lambda_1 f_1 \times \lambda_2 f_2$.

Errors in the rate estimates may have arisen from two assumptions that were made to expedite the analysis. First, β was fixed at 30000 s^{-1}, the value obtained from the saturation of the effective opening rate for many patches (Fig. 5). If the channel opening rate varied from patch to patch, or if the estimated saturation value is erroneous, then the other activation rate estimates may be biased. To examine the extent of these potential errors, fits were carried out where β was held constant at different values, from 15000 to 55000 s^{-1}.

Figure 13 shows the results from one model and one data file (the concerted model of Fig. 8), where the estimated rates of closing, association, and dissociation have been normalized to their values at 35000 s^{-1}. Over this range of β, the estimated association and dissociation rates change by less than $\pm 50\%$. Moreover, because

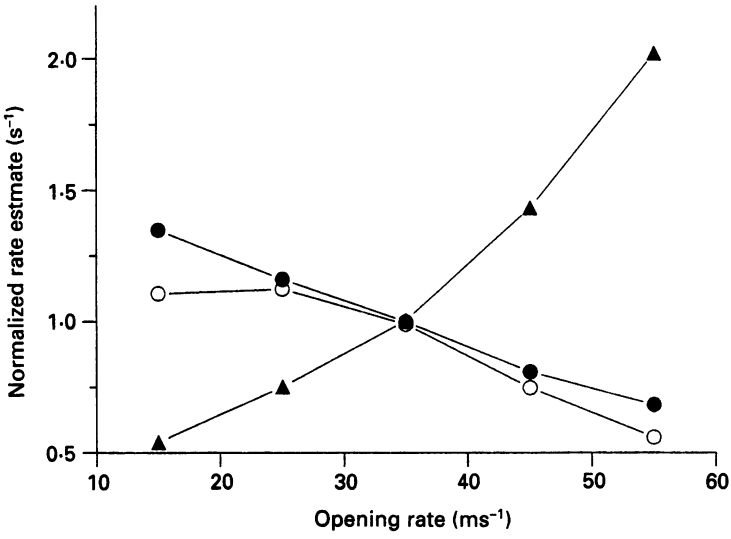

Fig. 13. Dependence of the rate estimates on the magnitude of the opening rate, β. The opening rate was fixed at the indicated value, and the remaining rates estimated by maximum-likelihood optimization (stepwise model; see Fig. 8). Only the closing rate estimate (▲) is strongly influenced by the chosen value of β, with association (●) and dissociation (○) rates changing < 1·5-fold.

both k_+ and k_- change in the same direction, the estimated K_d is even more weakly influenced by the chosen value of β. The opening rate, however is more strongly dependent on the value of β that was used for the fit, increasing markedly with higher values of β. Because the rates must support a constant apparent open channel lifetime, a faster opening is accompanied by a faster closing rate, but with more missed events. Thus, forcing the opening rate to be 30000 s^{-1} may have introduced a significant error in the closing rate estimate, but did not introduce large errors in the binding rate constant estimates.

A second potential bias in the analysis is the use of the simplified linear stepwise scheme (model (3)) rather than the fuller cyclic form (model (4)). This simplification is tantamount to assuming that $[A]k_+ < \beta_1$ and that $\beta_1 < k_-$. To test for errors introduced by using the linear scheme, the 100 μM backfilled pipette experiment shown in Fig. 11 (in which ACh concentrations up to 64 μM were analysed) was fitted both to models (3) and (4) (no symmetry; five free parameters). The rates estimated from the fit to the linear version of the stepwise model are given in Table 1C (top row); the rates from the fit to the cyclic version of the stepwise model were (s^{-1} or $\mu M^{-1}\ s^{-1}$): $k_+ = 239$, $k_- = 23158$, $\beta_1 = 12023$, $\alpha_1 = 3369$, and $\alpha = 670$. These values are consistently lower than those from the fit to the linear version, but are within

about a factor of 1·5. Because the discrepancy between linear and cyclic model parameters is greater at higher ACh concentrations, this result suggests that the use of the linear form of the stepwise model biased the rate estimates less that 1·5-fold.

In addition to inaccuracies introduced from assumptions in the analysis, in any fit there are standard errors associated with the parameter estimates. The magnitudes

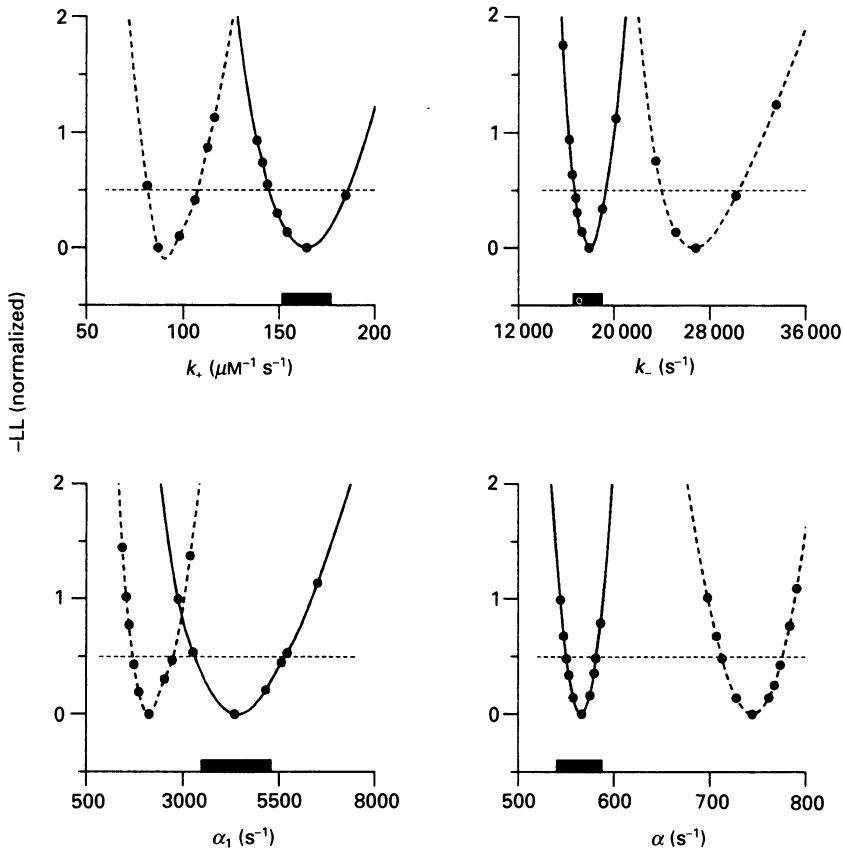

Fig. 14. Standard errors estimated by 0·5-unit likelihood intervals. Likelihood profiles were obtained by holding each rate to the indicated value and then optimizing according to the stepwise model (four parameters) to obtain the maximum log likelihoods (LL). Curves are cubic spline fits to ten to thirty such estimates (dashed line: 5 μM ACh file of Figs 7–10; continuous line: pipette backfilled with 10 μM ACh). The thin dashed line is the 0·5-unit likelihood level, at which point the width of the likelihood curve is equal to the standard error of the rate. For comparison, the bar on the abcissa is $\pm$one standard deviation, obtained by resampling the backfilled pipette experimental data 430 times. The 0·5-unit likelihood intervals and the resampling estimates of standard errors are similar, and are generally $< 25\%$ of the means.

of the standard error were probed both by the calculation of likelihood intervals (Colquhoun & Sigworth, 1983), and by resampling methods (Horn, 1987). Likelihood curves for two data files are shown in Fig. 14 (stepwise model four free parameters). In general, the 0·5 unit likelihood intervals for each parameter (equal to 1 S.E.M.) were

about 20% of the means. For example, in one patch the mean rates (+S.E.M., −S.E.M.) were $k_+ = 153$ (+28·4, −16·4), $k_- = 17830$ (+2150, −1520), $a_1 = 3557$ (+1480, −1030), and $\alpha = 567$ (+114, −70). The standard errors were larger with some rates than with others. In this file the average deviation was 20·4% of the mean, with the error limits on α_1 being largest (41%).

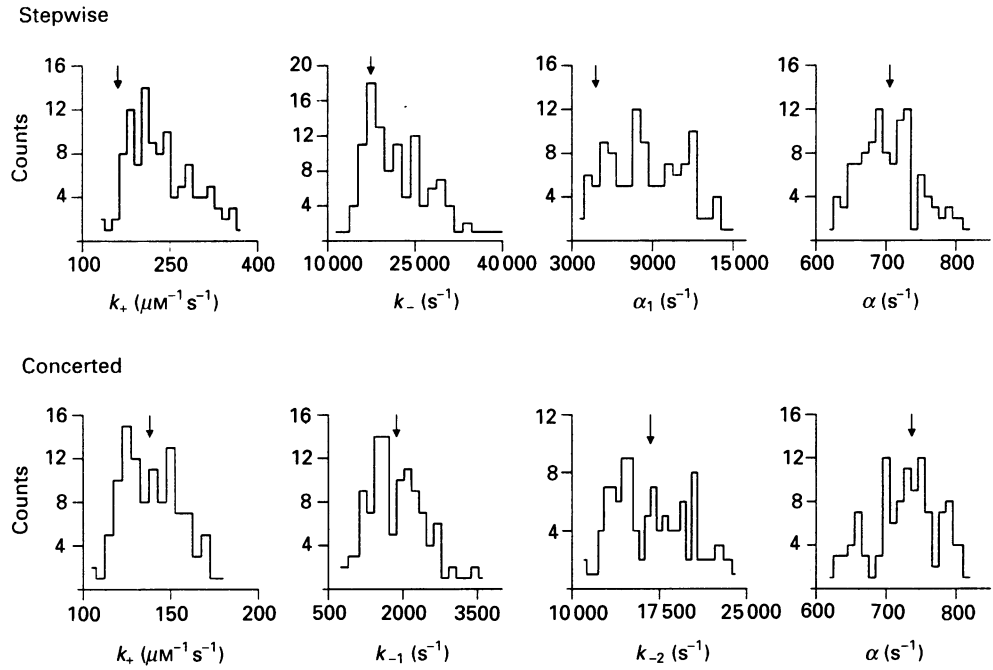

Fig. 15. Standard errors estimated by resampling. The 100 μM backfilled patch experiment (Fig. 11) was resampled and fit (110 cycles) to the four-parameter versions of stepwise and concerted models, producing these distributions of parameter estimates. The arrows indicate the rate estimates for the original interval list. Certain rates had broader distributions than others (i.e. α_1 by the stepwise model and k_{-2} by the concerted model).

As a second method of estimating parameter standard errors, three files were subjected to many cycles (30–430) of sampling and fitting (stepwise and concerted models) and the distributions of fitted rate constants were compiled. Figure 15 shows the rate estimate distributions for a four-parameter fit to the 100 μM backfilled patch experiment shown in Fig. 11, resampled 100 times. In each histogram, the arrow indicates the rate estimate from the original data set. As with the likelihood interval method, the standard deviations were within about 25% of the means, ranging from a low of 5% (α, either model) to a high of 36% (α_1, stepwise model). The similarity of the S.E.M. estimates by likelihood interval and resampling methods can be seen in Fig. 14, where the filled bars are ± 1 S.E.M. obtained by resampling and are similar in magnitude to the 0·5-unit likelihood interval.

The ability to garner accurate parameter estimates, and to distinguish between models, diminishes as the number of free parameters in the model increases. The effect can be quantified by the estimates of parameter standard errors that were

obtained by resampling under different constraints of symmetry. As expected, the accuracy of the rate estimates decreased as the number of free parameters in the fit increased. For one file (Figs 8–10) fitted by the fully symmetric, three-parameter versions of the stepwise and concerted models, the standard error of the rates averaged ~ 6% of the means (range : 4·5–6·8%). For the four-parameter version, the standard errors increased to ~ 17% of the means (range: 8·2–29·0%), and for the five-parameter version, they increased to ~ 23% of the means (range: 11·9–36·7). The magnitude of the errors were similar for both stepwise and concerted models. Not all rates were equivalent with regard to the increase in standard error with the number of parameters, as the variances of the association and dissociation rate distributions increased more markedly with added free parameters.

The results of these error analyses may be summarized as follows. The simplifying assumptions that were part of the analysis – fixing the value of β and using a linear rather than cyclic reaction scheme – may have biased the rate estimates, but probably by less than a factor of 1·5. In addition, the standard errors were different for each rate, but in general were < 25% of the mean estimates. With some exceptions, most notably in the closing rate, the scatter in the rate estimates given in Table 1 are within these limits, suggesting that the channel population was kinetically homogeneous.

Model selection by log likelihood ratios

There are no clear features of the data – the current records, the interval duration histograms, or the dose–response profiles – to forcefully guide the selection of the more appropriate kinetic scheme. Rather, I must rely on the LLR values given in Table 1 as the indicators of model superiority. These are rather abstract quantities, and it is therefore important to establish the weight that can be given to their magnitudes.

Sampling and bandwidth limitations, as well as the missed event correction, place limits on the analysis that are not readily quantified. Simulation was used to test whether stepwise and concerted models (with rates that are relevant to myocyte AChR) are indeed distinguishable (Horn, 1987). Current intervals ($n = 2500$) were simulated according to average rates of the four-parameter versions of either the stepwise or the concerted scheme, using sampling intervals (20 μs), noise levels (0·6 pA root mean square with a channel amplitude of 4 pA), bandwidths (5 kHz), burst durations (200 ms), and missed event corrections ($\tau_{dead} = 35$ μs) that were typical of the experiments. These simulated data sets were each fitted to stepwise and concerted kinetic schemes (four free parameters), and a LLR was computed. This procedure was repeated 100 times, and the resulting LLR values were compiled into the histograms shown in Fig. 16. Recall that a positive LLR indicates that the stepwise model fitted the data better than did the concerted model.

Clearly, stepwise and concerted models are distinguishable. When the simulation was according to the stepwise scheme, LLR values were mostly positive (mean = +2·0; S.D. = 1·55). When the simulation was according to the concerted scheme, LLR values were mostly negative (mean = −1·54; S.D. = 2·13). Both means are different from zero, and from each other, so the models are distinguishable. Moreover, although the absolute magnitude of the −LL for each fit was ~ 11000,

under the conditions of the simulation, detection, and fit, 'small' LLR values allow a clear selection between models. For example, a LLR value of -1·54 would indicate that the stepwise model was e-fold more likely than the concerted model, and a LLR of only −0·36 would indicate the converse. In Fig. 16, the arrowheads mark the boundaries where one model is 10 times more likely than the older.

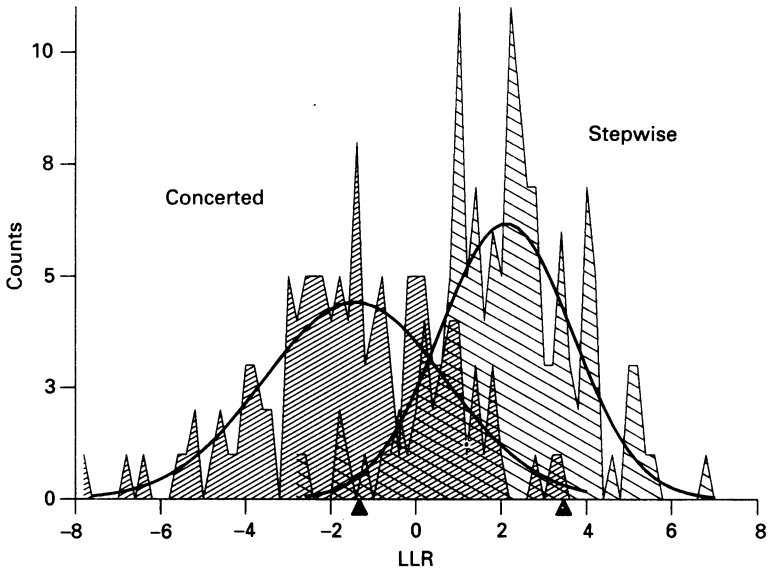

Fig. 16. Stepwise and concerted models are distinguishable. Currents were simulated (n = 100) according to the average rates (Table 1 B) of either the stepwise (light hatch) or concerted models (dark hatch), and were analysed by the same methods that were applied to experimental currents. A log likelihood ratio (LLR) was computed for each simulated data set by fitting to both stepwise and concerted schemes. A positive LLR indicates that the stepwise model fit better, and a negative LLR indicates that the concerted model fit better. On a population basis, the data were better fitted by the model that was used in the simulation. The arrowheads indicate LLR values that were 10 times more likely to come from one of the distributions, i.e. that would indicate that one model fitted 10 times better than the other.

The significance of the LLR values obtained from experimental data (Table 1) was examined by resampling. Artificially generating many 'new' data sets by resampling the original list of interval durations, and then fitting these to different models, produces a distribution of LLR values. A non-zero mean of this distribution indicates that one or the other model provides a better fit to the data. Note, however, that both the mean and variance of the LLR distribution will be biased if the original data is biased, thus this method must be considered to be an optimistic indicator of LLR significance.

The distributions of LLR values for a comparison of four-parameter stepwise *vs.* concerted models has been computed for the three patches that had the largest number of intervals (first three rows of Table 1 B). The results are shown in Fig. 17, where the original LLR is indicated by an arrow. The LLR distributions are approximately Gaussian, with means that are greater than zero: +11·0, +10·9, and

+28·0. Thus, in all three files the stepwise model fitted the population of resampled data sets better than did the concerted model. In order to develop a more intuitive appreciation of the significance of LLR values, it is useful to consider the magnitudes of the standard deviations of these distributions. Although the LL values for each fit

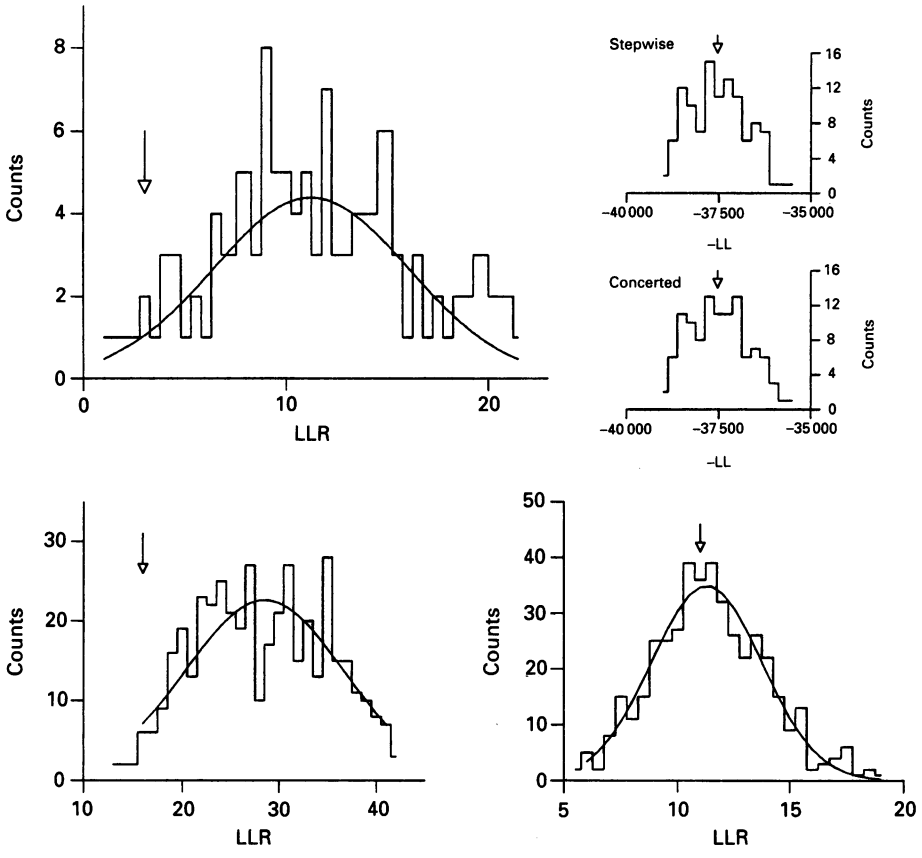

Fig. 17. Distributions of log likelihood ratios (LLR) obtained by resampling. The three files with the largest number of intervals (n = 2667, 4435, and 6776; see first three rows of Table 1 B) were resampled and fitted by four-parameter versions of both stepwise and concerted schemes. Three panels show the resulting LLR distributions; in upper right are LL distributions for stepwise and concerted fits to one file (upper left panel). The LLR values from fitting the original data set are indicated by the arrow. In all three files, the LLR distribution mean is positive, indicating a superior fit by the stepwise activation scheme.

were quite large (11000–38000), the standard deviations on the LLR distributions were rather small: 2·5, 4·8 and 8·2. Thus a LLR of only a few units can be a significant indicator of model superiority.

DISCUSSION

Model-independent conclusions

There are four strong conclusions that can be drawn regarding the activation rates of cholinergic channels in *Xenopus* myocytes. (1) Once doubly liganded, channels become conductive rapidly, at a rate of at least 25000 s^{-1}. (2) The agonist binding rate is fast, $\sim 2 \times 10^8$ M^{-1} s^{-1}, and approaches the limit set by diffusion. (3) The rate of dissociation of ACh from a doubly liganded channel is also fast, ~ 28000 s^{-1}. (4) There is an asymmetry in the activation process, i.e. binding to and/or gating of the two domains is not equivalent and independent. These conclusions are valid regardless of whether activation is by a stepwise or concerted mechanism.

The opening rate

The effective opening rate appears to saturate at 25000 s^{-1} (fetal-type channels, 18 °C, −120 mV). This value is in good agreement with the β value reported by Rohrbough & Kidokoro (1990) from an analysis of gaps within bursts at very low ACh concentrations in *Xenopus* myocytes of similar age (26400 s^{-1} at 14 °C, −175 mV). Although acquired by different experimental methods, opening rate estimates of similar magnitude have been reported for a number of preparations, including the frog endplate (gap characteristics at low ACh concentrations; Colquhoun & Sakmann, 1985), lizard endplate (endplate current rise time; Land, Salpeter & Salpeter, 1982), *Torpedo* receptors expressed in fibroblasts (low concentration analysis; Sine *et al.* 1990), and mouse BC_3H_1 cells (concentration jumps on excised patches; Liu & Dilger, 1991).

The experiments at high agonist concentrations unambiguously set a lower limit on the opening rate, but are consistent with still higher β values. With $\beta = 40000$ s^{-1}, the rates of the stepwise model predict a saturation limit of the effective opening rate of ~ 26000 s^{-1}, certainly consistent with the data shown in Fig. 5, as well as low concentration gap parameters that are in agreement with the values reported by Rohrbough & Kidokoro (1990).

While fast opening may be the rule for neuromuscular-type ACh receptors, there will undoubtedly be exceptions. Auerbach & Lingle (1986) have reported bursts with a low probability of being open at high ACh concentrations, and the opening rate of these forms of nicotinic channel are not known. Also, there is a substantial scatter in the *Xenopus* β' values at very high concentrations (Fig. 5), some of which may arise from intrinsic differences in the opening rate.

The association rate

Regardless of the model used to interpret the single channel current data, the ACh association rate is very fast and is close to being diffusion limited. This, too, appears to be a general characteristic of many kinds of nicotinic receptor, and is consistent with agonist binding sites that are accessible to the extracellular solution, or that are near fixed charges that serve to increase the local ACh concentration.

The dissociation rate

The rate at which ACh escapes from doubly liganded channels is quite rapid and is approximately equal to the opening rate, i.e. ~ 30000 s^{-1}. This means that for all

models, the second ACh molecule to bind does so with a low affinity, ~ 100–150 μM. Second agonist affinities in the mM range have been reported by Jackson (1989) and Sine *et al.* (1990). As discussed by Jackson (1988), the agonist must dissociate rapidly from the doubly liganded channel in order to allow a rapid termination of the synaptic current.

Activation asymmetry

The data indicate that in fetal-type neuromuscular receptors, the activation process is asymmetric. This asymmetry reflects differences in binding sites and/or gating domains. From the perspective of kinetics, time-invariant differences and co-operative interactions cannot be distinguished.

Interpretation of the activation rates

Muscle cell nicotinic AChR are composed of five homologous subunits: α, β, δ, and either γ or ϵ. The agonist binding sites lie at the α–γ (or α–ϵ) and α–δ subunit interfaces (Blount & Merlie, 1989; Pedersen & Cohen, 1990). Fluorescence energy transfer measurements indicate that they are > 3·5 nm apart (Johnson, Brown, Herz, Berman, Andreason & Taylor, 1989). If, as is postulated by the concerted scheme, permeation follows the removal of a single barrier (or the synchronous removal of several barriers) consequent to binding two agonists, then occupancy information (free energy) must be exchanged between the binding sites. This information transfer is not explicit in the concerted model, which therefore assumes that it is an unmeasurably fast, kinetically invisible event. In contrast, the stepwise scheme, which postulates the semiautonomous, sequential removal of the barriers to permeation, needs no additional assumptions and in this sense is simpler than the concerted scheme. If the hidden conformation change implicit to the concerted scheme were made explicit by the inclusion of an additional closed state between the two binding steps, the concerted and stepwise models would converge.

The regions of the δ and γ subunits that contribute to the binding sites (possibly near tryptophan 55; Chiara & Cohen, 1992) are likely to have different residues and it is therefore reasonable to suppose that the sites have different affinities for agonists. The two agonist binding sites indeed do have more than 10-fold different apparent binding affinities for carbamylcholine (Blount & Merlie, 1989), although this conclusion is based on equilibrium binding to desensitized receptors that would certainly convolve binding and isomerization rates. Also, Pedersen & Cohen (1990) have reported that the α–γ binding site has an affinity for *d*-tubocurare that is 20–35 times higher than that of the α–δ site. Note that according to eqn (4), the average stepwise rates of Table 1C predict a 36-fold difference in the apparent affinity of the two domains for ACh. To limit the number of free parameters in the fit, I have made the assumption that in the stepwise model, the binding sites are equivalent. The stepwise model can readily accommodate different agonist binding affinities, and it is important to emphasize that stepwise activation in no way implies equivalent sites. Without more extensive data records, a statistical test of the value of making the sites non-equivalent is not yet possible.

With the concerted model, allowing the binding rate constants to differ for the two association steps significantly improves the fit, with the major difference being an increase in the dissociation rate at one site. According to the average rates concerted

scheme (Table 1C), there is about a 8-fold decrease in the affinity at the second site relative to the first. Similar, but more extreme, negative co-operativity has been previously reported by Jackson (1989) in mouse receptors and Sine *et al.* (1990) in *Torpedo* receptors. With the stepwise model, the asymmetry of the activation process is manifest mostly as a difference in the closing rate of the two gating domains. The kinetic analysis does not distinguish between non-identical, independent domains (i.e. a static difference in gating kinetics) and identical, dependent domains (i.e. dynamic interactions between domains).

On average, there is about a 12-fold difference in the deactivation rate and a 3-fold difference in the activation rate between domains. According to the stepwise view, in the example file of Fig. 9 activation asymmetry is manifest as about a 20-fold increase in the activation/deactivation rate ratio (from 4·6 to 93) between the first and second gating steps. With either the static or dynamic mechanistic interpretation of the rates, the effect of this pattern is to stabilize both the vacant–closed and open conformations of the channel, i.e. the extremes of the reaction sequence, while destabilizing the reaction intermediates.

That the binding sites lie at the interface between α–δ or α–γ polypeptides suggests that a subunit pair constitutes a gating domain. With stepwise gating, after binding an ACh molecule, the α plus either δ or γ subunits change their conformations as a single unit (rates β_1 or β) so as to remove some barriers to ionic permeation. Interestingly, the aspartate receptor of *Escherichia coli* binds ligand at the interface between two identical subunits which shift their relative conformations as a consequence of such binding (Milburn, Prive, Milligan, Scott, Yeh, Jancarik, Koshland & Kim, 1991). The AChR β subunit does not participate in agonist binding, but neither may it offer a significant barrier to ion flow (Villaroel, Herlitze & Sakmann, 1992).

Concerted vs. stepwise models

Several criteria can serve to guide the selection between alternative models, e.g. plausibility, precedent, and statistics. Concerted and stepwise kinetic schemes have been considered in detail with regard to haemoglobin and enzyme activation for some time, and both models are plausible mechanisms of protein operation (Ackers, Doyle, Myers & Daugherty, 1992; see Wyman & Gill, 1990). Moreover, the molecular basis of gating in the superfamily of ligand-dependent channels is still unknown, so the rule of precedent cannot be brought to bear on the choice of a kinetic scheme. The remaining criterion for model selection, statistics, favours the stepwise scheme.

First, for the nine patches that were analysed, the stepwise model consistently fitted the interval data better than did the concerted model (as evidenced by the positive LLR values given in Table 1). In a file-by-file comparison of the two models, and with each file treated identically (number of events, number of free parameters, dead time, and optimization criteria), the stepwise model was the more likely in 67 % of the cases. If fits that assumed full symmetry (equal and independent binding or gating) are discarded from this accounting, then only three of eighteen comparisons were better described by the concerted scheme, with these being files having relatively few intervals (i.e. broad LLR distributions). The aggregate likelihood, too, was greater for the stepwise model under the assumptions of full (LLR = +12),

partial (LLR = +46), or no symmetry (LLR = +24) in the activation process. Finally, simulation (Fig. 16) and resampling (Fig. 17) results suggest that the positive values of the LLRs in files which had at least 2500 intervals were significant.

Overall, the statistical analysis of the single channel kinetics suggest that for *Xenopus* myocyte fetal-type ACh receptors, stepwise activation is as good as or better than the traditional concerted scheme. This conclusion must be tempered because relatively few files were analysed, many rates were near the bandwidth limit of the system, the behaviour of the missed event correction is poorly understood, and kinetics alone cannot prove that a model is that one that corresponds to the physical reality. More extensive kinetic analyses, and corollary evidence from biochemical, pharmacological, molecular biology, and structural experiments, must be brought to bear on the discrimination between stepwise *vs.* concerted activation of multimeric proteins.

Ancillary support for the stepwise model

Dose–response profiles

The higher conductance, adult class of cholinergic channel that is present on late stage myocytes closes about 5 times faster than does the fetal-type channel (Rohrbough & Kidokoro, 1990). In addition to having a larger conductance and a shorter open channel lifetime, adult channels show a clear rightward shift in its dose–response profile relative to fetal channels, also by about a factor of 5 (Auerbach & Lingle, 1987). Thus the half-maximal P_o is a 5 μM ACh for fetal channels and 25 μM ACh for adult channels. This shift in dose–response profile may be considered in the light of the stepwise model.

If we assume that the ACh association rate is the same for both conductance classes of channel, then eqn (4) can be used to compute the relative shift in the effective equilibrium dissociation constant (K^*) between adult (A) and fetal (F) receptors:

$$\frac{K^*_A}{K^*_F} = \frac{\alpha_A}{\alpha_F}\frac{\beta_F + \alpha_F}{\beta_A + \alpha_A},$$

where β and α are the activation and deactivation rates of the first gating domain. Under the condition that the sums of the isomerization rates are similar for the two classes of channel (for example, if $\beta_F = \beta_A > \alpha_F$ and α_A), then the apparent shift in affinity is equal to the ratio of domain inactivation rates, α_A/α_F.

Although the activation rates for the adult-type channel according to the stepwise model are unknown, the fetal-type channel might appear to have a higher affinity simply because of a slower deactivation rate. That is, in fetal-type channels there is a shift in the gating isomerization equilibrium that both keeps the channel open and 'traps' agonist in the binding site. The observed decrease in the apparent affinity of adult-type channels relative to fetal-type channels can be quantitatively accounted for by the stepwise model without any modification in the association or dissociation rates.

Temperature dependence of rates

Sine *et al.* (1990) have reported a surprisingly high temperature coefficient (Q_{10}) for agonist dissociation in *Torpedo* receptors expressed in fibroblasts. Again, the stepwise model predicts that the apparent Q_{10} of dissociation is influenced by the single-

domain isomerization rates. If $\beta_1 > \alpha_1$, the apparent Q_{10} of the dissociation rate ($Q^*_{k_-}$) can be computed from eqn (4):

$$Q^*_{k_-} = \frac{Q_{k_-} Q_{\alpha_1}}{Q_{\beta_1}}.$$

where Q_{k_-}, Q_{α_1}, and Q_{β_1} are the Q_{10} values of the dissociation, inactivation, and activation rates. Thus, if the slower inactivation rate is more temperature sensitive than the activation rate, the apparent Q_{10} of dissociation will be higher than the true value. That is, if a stepwise process were analysed according to a concerted scheme, the apparent Q_{10} of k_- would be of the product of Q_{10} values of one or more rates.

Spontaneous openings

In my experiments, the bandwidth was too low and the ACh concentration too high to make monoliganded openings a significant feature of the current record. Spontaneous and monoliganded openings can be incorporated into the stepwise model by assuming a low activation rate (β_0) and a fast inactivation rate (α_0) of a gating domain with no ligand bound:

$$C_1 \underset{\alpha_0}{\overset{2\beta_0}{\rightleftharpoons}} C_2 \underset{2\alpha_0}{\overset{\beta_0}{\rightleftharpoons}} O.$$

If brief openings at low agonist concentration are monoliganded receptors, then, because Kidokoro & Rohrbough (1990) report the lifetime of fetal-type AChR brief openings to be ~ 64 μs, $\alpha_0 = 7800$ s^{-1}. This is about twice as fast as the estimated inactivation rate of the first liganded subunit (3400 s^{-1}), according to the stepwise model. Using Jackson's (1988) estimate that $\beta/\beta_0 = 10^4$, model (5) predicts spontaneous openings at a rate of 0·002 s^{-1} per channel. Kidokoro & Rohrbough observed a spontaneous opening rate of about 0·2 s^{-1} (three patches), a rate that would be expected to be generated by a patch with 100 channels. This value is of the correct order of magnitude, and, given the rough rate estimates, suggests that a stepwise gating scheme is consistent with the observed frequency of spontaneous openings.

Agonist trapping

Both the concerted and stepwise models postulate that activation prevents the escape of agonist. In support of this notion, the kinetic parameters derived from an analysis of gaps at low ACh concentrations (which would disappear if agonist could readily escape the open channel) agree with kinetic parameters gained from high concentration experiments.

If the rate of ACh dissociation from doubly liganded channels is fast and the maximum for the ligand association rate is set by diffusion (i.e. the receptor has a low affinity for ACh), opening channels at agonist concentrations far below the equilibrium dissociation constant is a problem. According to the concerted view, this is accomplished by making the affinity of one binding site substantially higher than that of the other (Jackson, 1988; Sine *et al.* 1990). According to the stepwise view, the problem is solved by coupling the conformational change that constitutes domain activation (and is necessary for ion conduction to occur) to one that prevents

the escape of the agonist from its binding site. For both models, the result is a shift of the dose–response profile towards lower agonist concentrations at the expense of a reduction in the apparent co-operativity of the overall response.

Numerous enzymes encapsulate substrate. In the case of triosephosphate isomerase, crystallographic studies (Lolis & Petsko, 1990) in combination with molecular dynamic simulations (Joseph, Petsko & Karplus, 1990), indicate that consequent to binding ligand, an eleven-residue loop region (a 'hinged lid') moves to trap the ligand in the catalytic site. Pompliano, Peyman & Knowles (1990) have suggested that the functional role of this manoeuvre is to trap reaction intermediates thus increasing the net catalytic rate, while Lolis & Petsko (1990) argue that the lid serves to exclude bulk water thereby increasing the electrostatic interactions that drive catalysis. More germane to AChR, the three-dimensional structure of the ligand-binding region of the aspartate receptor has been solved (Milburn *et al.* 1991), and the shift between subunits that accompanies aspartate binding appears to trap the ligand in its site. Although the conformational correlates and rationale for agonist trapping in receptors for small ligands is less clear than in enzymes, the structural changes in AChR that result in agonist trapping and ion permeation may be considered to be 'tightly' coupled because the opening rate is $\sim 30000\ s^{-1}$.

The stepwise view

The following is one possible picture of ACh receptor activation that emerges from the rates of the stepwise kinetic model (fetal channels, −120 mV, 18 °C).

ACh receptors have two gating domains, each with a site that binds ACh. These sites span α–δ and α–γ subunits, thus α–δ and α–γ couplets may be considered to be the salient domains. In the vacant, quiescent channel these domains may perhaps be symmetric, i.e. the two binding sites and 'gates' may each be equivalent, but interact with each other during activation. Alternatively, two non-equivalent domains may activate independently. The following description pertains to stepwise activation by interacting domains.

Activation begins when an ACh molecule binds to one of the sites at a rate that is nearly diffusion limited. The ACh molecule remains there only a short time, 15–30 μs, before something happens. Usually ($\sim 70\%$ of the time), it simply dissociates. This is a reflection of the low intrinsic affinity of the site for its transmitter ($K_d = 130\ \mu M$). Less frequently, the occupied domain shifts to a conformation that both 'traps' ACh in its binding site, and is necessary but not sufficient for ionic permeation. If, during this time, the counterpart domain remains unactive, the structure will return to its resting conformation within $\sim 350\ \mu$s. If, however, during this time the counterpart domain also binds ACh and becomes active, the remaining barriers to permeation are removed and ionic conduction occurs. Now, the domain deactivation rate is slowed about 10-fold relative to that of the half-activated channel and current flows until one domain deactivates, i.e. for $\sim 1{\cdot}8$ ms. In a synaptic current, where the concentration of ACh is rapidly reduced to nil by enzymatic and diffusive forces, after a channel closes it can either reopen, lose an agonist, or oscillate between two doubly liganded states (both domains resting or one resting and one active). Thus, the stepwise model predicts that the rate of synaptic current decay will be described by three exponentials with characteristic time constants that are governed by five

kinetic processes: the activation and deactivation rates of the two domains, and the rate of agonist dissociation.

I wish to thank Dick Horn for generously providing his source code to compute the likelihood function. I also thank Xun Sun, Bo Cen, Bing Liu, Yang He, and Zhonqui Jing for excellent computer programming, and Mary Gauthier-Teeling, Diane Pickersgill and Robert Borschel for technical assistance. Finally, I thank Bernard Katz, Karl Magleby, and Chris Lingle for their comments on the manuscript. Supported by NS23513 from the National Institutes of Health and BNS-9102232 from the National Science Foundation.

REFERENCES

ACKERS, G. K., DOYLE, M. L., MYERS, D. & DAUGHERTY, M. A. (1992). Molecular code for cooperativity in hemoglobin. *Science* **255**, 54–63.

AUERBACH, A. (1991). Single-channel dose–response studies in single, cell-attached particles. *Biophysical Journal* **60**, 660–670.

AUERBACH, A. (1992). ACh receptor subunits in *Xenopus* myocytes activate semi-autonomously. *Biophysical Journal* **61**, A105.

AUERBACH, A. & LINGLE, C. J. (1986). Heterogeneous kinetic properties of acetylcholine receptor channels in *Xenopus* myocytes. *Journal of Physiology* **378**, 119–140.

AUERBACH, A. & LINGLE, C. J. (1987). Activation of the primary kinetic modes of large- and small-conductance cholinergic ion channels in *Xenopus* myocytes. *Journal of Physiology* **393**, 437–466.

BATES, S. E., SANSOM, M. S. P., BALL, F. G., RAMSEY, R. L. & USHERWOOD, P. N. R. (1990). Glutamate receptor-channel gating. *Biophysical Journal* **58**, 219–229.

BLOUNT, P. & MERLIE, J. P. (1989). Molecular basis of the two nonequivalent binding sites of the muscle nicotinic acetylcholine receptor. *Neuron* **3**, 349–357.

CHIARA, D. C. & COHEN, J. B. (1992). Identification of amino acids contributing to high and low affinity D-tubocurarine (dTC) sites on the *Torpedo* nicotinic acetylcholine receptor (nAChR) subunits. *Biophysical Journal* **61**, A106.

COLQUHOUN, D. & HAWKES, A. G. (1977). Relaxation and fluctuations of membrane currents that flow through drug-operated channels. *Proceedings of the Royal Society* B **299**, 231–262.

COLQUHOUN, D. & HAWKES, A. G. (1982). On the stochastic properties of bursts of single ion channel openings and of clusters of bursts. *Philosophical Transactions of the Royal Society* B **300**, 1–59.

COLQUHOUN, D. & OGDEN, D. C. (1988). Activation of ion channels in the frog end-plate by high concentrations of acetylcholine. *Journal of Physiology* **395**, 131–159.

COLQUHOUN, D. & SAKMANN, B. (1985). Fast events in single-channel currents activated by acetylcholine and its analogues at the frog muscle end-plate. *Journal of Physiology* **369**, 501–557.

COLQUHOUN, D. & SIGWORTH, F. J. (1983). Fitting and statistical analysis of single-channel records. In *Single-Channel Recording*, ed. NEHER, E. & SAKMANN, B. Plenum Press, New York.

CROUZY, S. C. & SIGWORTH, F. J. (1990). Yet another approach to the dwell-time omission problem of single-channel analysis. *Biophysical Journal* **58**, 731–743.

DEL CASTILLO, J. & KATZ, B. (1957). Interaction at end-plate receptors between different choline derivatives. *Proceedings of the Royal Society* B **146**, 369–381.

DIONNE, V. E. (1976). Characterization of drug iontophoresis with a fast microassay technique. *Biophysical Journal* **16**, 705–717.

FATT, P. & KATZ, B. (1952). Spontaneous subthreshold activity at motor nerve endings. *Journal of Physiology* **117**, 109–128.

HODGKIN, A. L. & HUXLEY, A. F. (1952). A quantitative description of membrane current and its application to conduction and excitation in nerve. *Journal of Physiology* **117**, 500–544.

HORN, R. (1987). Statistical methods for model discrimination. *Biophysical Journal* **51**, 255–263.

HORN, R. & LANGE, K. (1983). Estimating kinetic constants from single channel data. *Biophysical Journal* **43**, 207–223.

HORN, R. & VANDENBERG, C. A. (1984). Statistical properties of single sodium channels. *Journal of General Physiology* **85**, 505.

JACKSON, M. B. (1986). Kinetics of unliganded acetylcholine receptor channel gating. *Biophysical Journal* **49**, 663–672.

JACKSON, M. B. (1988). Dependence of acetylcholine receptor channel kinetics on agonist concentration in cultured mouse muscle fibres. *Journal of Physiology* **397**, 555–583.

JACKSON, M. B. (1989). Perfection of a synaptic receptor: kinetics and energetics of the acetylcholine receptor. *Proceedings of the National Academy of Sciences of the USA* **86**, 2199–2203.

JOHNSON, D. A., BROWN, R. D., HERZ, J., BERMAN, H. A., ANDREASON, G. L. & TAYLOR P. (1989). Decidium: a novel fluorescent probe of the agonist/antagonist and noncompetitive inhibitor sites of the nicotinic acetylcholine receptor. *Journal of Biological Chemistry* **262**, 14022–14029.

JOSEPH, D., PETSKO, G. A. & KARPLUS, M. (1990). Anatomy of a conformational change: hinged "Lid" motion of the triosephosphate isomerase loop. *Science* **249**, 1425–1428.

KATZ, B. & THESLEFF, S. (1957). A study of the 'desensitization' produced by acetylcholine at the motor end-plate. *Journal of Physiology* **138**, 63–80.

KIDOKORO, Y. & ROHRBOUGH, J. (1990). Acetylcholine receptor channels in *Xenopus* myocytes culture: brief openings, brief closures and slow desensitization. *Journal of Physiology* **425**, 227–244.

KOSHLAND, D. E. JR, NEMETHY, G. & FILMER, D. (1966). Comparison of experimental binding data and theoretical models in proteins containing subunits. *Biochemistry* **5**, 365–385.

LAND, B. R., SALPETER, E. E. & SALPETER, M. M. (1981). Kinetic parameters for acetylcholine interaction in intact neuromuscular junction. *Proceedings of the National Academy of Sciences of the USA* **78**, 7200–7204.

LIU, Y. & DILGER, J. P. (1991). The opening rate of acetylcholine receptor channels. *Biophysical Journal* **60**, 424–432.

LOLIS, E. & PETSKO, G. A. (1990). Crystallographic analysis of the complex between triose-phosphate isomerase and 2-phosphoglycolate at 2·5-A resolution: implications for catalysis. *Biochemistry* **29**, 6619–6625.

MACONOCHIE, D. J. & STEINBACH, J. H. (1992). Adult and foetal acetylcholine receptor channel opening rates. *Biophysical Journal* **61**, A142.

MAGELBY, K. L. & WEISS, D. S. (1990). Estimating kinetic parameters for single channels with simulation. *Biophysical Journal* **58**, 1411–1426.

MILBURN, M. V., PRIVE, G. G., MILLIGAN, D. L., SCOTT, W. G., YEH, J., JANCARIK, J., KOSHLAND, D. E. JR & KIM, S. H. (1991). Three-dimensional structures of the ligand-binding domain of the bacterial aspartate receptor with and without a ligand. *Science* **254**, 1342–1347.

MONOD, J., WYMAN, J. & CHANGEAUX, J. P. (1965). On the nature of allosteric transitions: A plausible model. *Journal of Molecular Biology* **12**, 88–118.

NELDER, J. A. & MEAD, R. (1965). A simplex method for function minimization. *Computer Journal* **7**, 308–313.

NEIL, J., XIANG, Z. & AUERBACH, A. (1991). List-oriented analysis of single-channel data. *Methods in Neuroscience* **4**, 474–490.

NIEUWKOOP, P. D. & FABER, J. (1967). *Normal Table of Xenopus laevis, (Daudin)*. Elsevier/North Holland, Amsterdam.

OGDEN, D. C. & COLQUHOUN, D. (1985). Ion channel block by acetylcholine, carbachol and suberyldicholine at the frog neuromuscular junction. *Proceedings of the Royal Society* B**225**, 329–355.

PEDERSEN, S. E. & COHEN, J. B. (1990). *d*-Tubocurarine binding sites are located at the α–γ and α–δ subunit interfaces of the nicotinic acetylcholine receptor. *Proceedings of the National Academy of Sciences of the USA* **87**, 2785–2789.

POMPLIANO, D. L., PEYMAN, A. & KNOWLES, J. R. (1990). Stabilization of a reaction intermediate as a catalytic device: definition of the functional role of the flexible loop in triosephosphate isomerase. *Biochemistry* **29**, 3186–3194.

ROHRBAUGH, J. & KIDOKORO, Y. (1990). Changes in kinetics of acetylcholine receptor channels after initial expression in *Xenopus* myocyte culture. *Journal of Physiology* **425**, 245–269.

ROUX, B. & SAUVE, R. (1985). A general solution to the time interval omission problem applied to single channel analysis. *Biophysical Journal* **48**, 149–158.

SACHS, F., NEIL, J. & BARKAKATI, N. (1982). The automated analysis of data from single ionic channels. *Pflügers Archiv* **395**, 331–340.

SAKMANN, B., PATLAK, J. & NEHER, E. (1980). Single acetylcholine activated channels show burst-kinetics in the presence of desensitizing concentrations of agonist. *Nature* **286**, 71–73.

SIGWORTH, F. J. & SINE, S. M. (1987). Fitting and display of single channel dwell time histograms. *Biophysical Journal* **52**, 1047–1054.

SINE, S. M., CLAUDIO, T. & SIGWORTH, F. J. (1990). Activation of *Torpedo* acetylcholine receptors expressed in mouse fibroblasts: single channel current kinetics reveal distinct agonist binding affinities. *Journal of General Physiology* **96**, 395–437.

SINE, S. M. & STEINBACH, J. H. (1984). Agonists block currents through acetylcholine receptor channels. *Biophysical Journal* **46**, 277–284.

VILLARROEL, A., HERLITZE, S. & SAKMANN, B. (1992). Amino acids in the narrow region of the rat acetylcholine receptor channel. *Biophysical Journal* **61**, A142.

WYMAN, J. & GILL, S. J. (1990). *Binding and Linkage*. University Science Books, Mill Valley, CA, USA.